Title
ANALYSIS OF BUBBLE CHAMBER DATA

Authors
Humphrey, William E.
Rosenfeld, Arthur H.

Publication Date
1963-06-17

UCRL-10812

University of California

Ernest O. Lawrence Radiation Laboratory

ANALYSIS OF BUBBLE CHAMBER DATA

DISCLAIMER

UCRL-10812

UNIVERSITY OF CALIFORNIA

Lawrence Radiation Laboratory
Berkeley, California

Contract No. W-7405-eng-48

ANALYSIS OF BUBBLE CHAMBER DATA

William E. Humphrey and Arthur H. Rosenfeld

June 17, 1963

Submitted to Annual Review of Nuclear Science, 1963.

ANALYSIS OF BUBBLE CHAMBER DATA

Contents

Contents

ANALYSIS OF BUBBLE CHAMBER DATA*

William E. Humphrey and Arthur H. Rosenfeld

Lawrence Radiation Laboratory and Department of Physics,
University of California, Berkeley, California

June 17, 1963

INTRODUCTION

There are currently in operation several different systems for processing bubble chamber data, most of which perform very much the same functions, and most of which have common origins. They have all been described at two 1962 conferences, the Conference on Instrumentation for High Energy Physics held at CERN (1) and an informal conference that followed it (2). In this article, rather than comparing different current systems, we have tried to write for the graduate student or experimental physicist who is contemplating his first bubble chamber experiment. The choice of which system he uses (one from Berkeley, Brookhaven or Yale, CERN or Paris, etc.) is in general already determined by history and geography; he will be most interested in using the most readily available one, whichever that may be, to get meaningful results. So we have concentrated on the current system we know best, that of the Alvarez group at Berkeley. At the end of the article, where we take up various new systems for automatic measuring and automatic scanning, we do try to compare the competing approaches.

Returning to the matter of references, we would like to emphasize that reference 1 orovides an up-to-date 100-page source of information on high-energy physics data analysis, and we cannot attempt to summarize all the information that pertains to bubble chamber analysis in this 25-page article. Further, reference 3 (which is contained in reference 1) is referred to frequently in connection with the bubble chamber analysis for the Alvarez Group at Berkeley. We have referred to this article in preference to adding a list of about 20 reports and publications to the bibliography of this paper. Further general discussion of costs and future systems is found in the survey by Miller and Fulbright (4).

1. OUTLINE OF A CURRENTLY OPERATING SYSTEM

We chose here the 72-inch hydrogen bubble chamber system at Berkeley, with measurements made on Franckensteins.[5] During the 12 months preceding a Bevatron shutdown in June 1962, the chamber produced a million "triads" (triple stereo views). During this same time about 100 people in all (physicists plus technicians) recorded about 200,000 "interesting" events, and measured and processed about 100,000 of these. We shall now outline the procedures that were followed. For more details and a history of this system, see reference 3. (The following description represents one of the two major bubble chamber analysis systems in use at Berkeley. In addition to the Alvarez system described below, there is the well-known FOG-CLOUDY-FAIR analysis scheme developed by Howard S. White, which is described in reference 6.)

1.1 The scanning and measuring process.

The portion of bubble chamber analysis which actually deals with the photographs of the bubble chamber has so far been a two-step process. The first step is the scanning operation. The purpose of scanning is to provide a catalogue (master list) of interesting events, which can be called upon later for lists of roll and frame numbers of any events recorded during the scan. Scanning takes place on a special

high-quality projection table which is provided with a film-transport mechanism. The scanner records events on scanning forms according to instructions appropriate to the experiment being scanned, and key-punch girls transcribe the information from the scanning forms onto punched cards. Finally the scanning cards are merged onto a magnetic tape which serves as the master list for the entire experiment.

The second step in the film handling operation is the measurement process. The experimentalist defines a class of events that he wishes to measure. The locations of these events in the film are abstracted from the master list in the form of a measurement listing and measurement control cards. At this stage, film is mounted on one of the Franckensteins. The event is positioned for measurement by either manually positioning the film at the frame number on the measurement listing or (on the more highly automated Franckensteins) by slipping the measurement control card into a card-reading device which is capable of controlling the position of the film. The measurement control card also has on it information that is used to automatically position the stage at the vertex to be measured. The film is carried on a very precise heavy-duty microscope stage which is digitized in two orthogonal directions (x and y coordinates) to a least count of 2.54 microns. Two different images of the same view are visible to the Franckenstein operator. One is an overall view of the film and the other is a magnified view of a portion of the film, with a cross hair in the center. The region of the film in the vicinity of the cross hair on the magnified view is also seen by an electronic servo circuit. The operator measures a track by moving the microscope stage until the cross hair and track coincide. A servo system is then able to control the motion of the microscope stage in such a way that the track can be moved along its tangent at the cross hair, while at the same time, the track is kept centered to about the precision of the least count. The operator causes the values of the x and y digitizers to be recorded on magnetic or paper tape for every few millimeter of stage motion.

Special points such as fiducials or vertices may be measured by manually centering the point to be measured on the cross hair of the high-power screen. Various aids to the operator are built into Franckensteins. The measurement control card contains the approximate position of the vertex that is to be measured. The Franckenstein is able automatically to position the microscope stage near the vertex at the correct time in the measuring sequence, and similarly the stage is automatically positioned for fiducial measurements. View sequencing is also taken care of automatically. All three views of each track are measured, and the view number of each set of track measurements is carried along. (Recent changes in the track-analysis programs allow a track measurement in one view to be skipped if it does not appear to be required in the analysis.)

The track measurements may be put out onto paper tape, magnetic tape, or punched cards, depending on the particular measuring projector. As a last operation in the measuring process, the output from all measuring projectors is processed by the computer program PANAL, which reorganizes the data into a single magnetic tape format. PANAL carries out some simple tests on the data in order to cull out events that would fail in the later analysis programs, and compacts all the data for an entire event into a single record on tape.[1] PANAL is also used to order and merge measurement tapes. (Ordering is by film roll and frame number.) About 12,000 "event" measurements can be stored on a 2400-foot 800-character-per-inch tape (in PANAL output format). Figure 1 displays the role of PANAL and later programs; Table I summarizes their characteristics.

1.2 Stereo reconstruction.

The actual physics analysis of bubble chamber film starts with the reconstruction in space of the bubble chamber tracks. The information provided (by the measuring machine) for these calculations includes identification of the tracks measured (frame number, view number, etc.), measurements of points along tracks in several views, and measurements of fiducial marks on the film (which are used

to establish the frame of reference for the track measurements). Track measurements may also include additional information, such as whether or not the track stopped in the chamber, or bubble density information. The information resulting from the reconstruction usually includes the position, momentum, and orientation of each track at the end, and estimates for the uncertainties of these quantities.

The reconstruction process itself can be divided into two sections: first the geometrical reconstruction of points along the track, and second the fitting of the geometrically reconstructed points to an appropriate curve. There are various approaches to each of these problems. Early approaches are embodied in the current programs PANG, FOG and TRED(3, 6).

The PANG geometric reconstruction relies on the fact that if the film position of a given bubble on a track were known in two views, then tracing the light rays from the two views back through the optics into the bubble chamber would yield an intersection of rays at the position of the bubble. In actual practice, measurements are not made at corresponding points in the various views, and it is necessary to generate an artificial corresponding point in some view by interpolating between two measured points. The interpolation is simple in the case of an ideal lens system involving only distortion-free lenses, but the actual optics are usually far more involved. Some of the effects that must be taken into account are lens distortion, film shrinkage, tilted mirrors, thick glass windows, and the index of refraction of the liquid in the bubble chamber. As a consequence, the corresponding point is found by iterating once after a nearly corresponding point based on ideal optics has been found. This process is repeated for each measured point of a view to yield the space coordinates of a string of points that lie along a track. A curve is fitted to these points by the least-squares curve-fitting procedure. The PANG program makes use of two independent power series to form the following parameterization of a space curve:

$$y = y(x, a_1, a_2, a_3)$$

$$z = z(x, a_4, a_5), \qquad x = x.$$

The shapes of these fitting curves are constrained to take into account variations of magnitude and direction of the magnetic field, and changes in curvature resulting from energy loss along the track. These constraints take the form of correction terms which are included in the power series. The first three-parameter curve involving terms to the fourth power (cubic and quartic correction terms) is used to fit the track in its projection on a plane nearly normal to the magnetic field. The second two-parameter cubic curve (quadratic and cubic correction terms) is fitted to a projection on a plane which includes the chord of the track and (essentially) the magnetic field. The final angles and momenta at each end of the track are based on the parameters of these curves. The energy-loss correction requires knowledge of the particle mass, therefore the calculated track parameters are mass-dependent. When the identity of a track is ambiguous, it is customary to repeat the mass-dependent portion of the calculations for several mass hypotheses.

Estimates of the uncertainties in the central values of the track variables pose one of the most difficult problems in the reconstruction program. There are three main contributions to the total uncertainty for track variables. The first arises from the measurement uncertainty of the measuring device, the second contribution is from multiple Coulomb scattering, and the third corresponds to a general degrading of measurements due to miscellaneous "unpredictable" effects such as small errors in the optical constants, or plural scattering, or turbulence in the chamber. Both the Berkeley program PANG and the CERN track analysis program THRESH (8) follow basically the same procedure for estimating the uncertainty of the track variables. It is assumed that the measuring machines contribute some known measurement error in the film plane, transverse to the track direction. This point-scatter error is assumed to be a property of the measuring device which does not change from one track to another. This "known" point-scatter uncertainty (an "external error") in the film plane is propagated through the spatial reconstruction to form the first contribution to the uncertainty in the track variables. In actual practice, we

find it convenient to include some of the "unpredictable" errors in the point scatter, consequently the value we use is about twice the value that if would otherwise have. For each individual track it is possible to examine the scatter of points about a smooth fitted curve on the film and arrive at an estimate for the scatter of points (an "internal error") which may be compared with the external error. If there is a bad point causing an excessive internal error estimate, then either the point is discarded or the entire track view may be rejected. The internal error estimate is not used in estimating (for subsequent programs) the measurement uncertainties of the track variables because it is subject to statistical fluctuations from one track to the next. The multiple Coulomb scattering contribution is combined with the measurement contribution after both track reconstruction and fitting are complete, and the mass and momentum of the particle are available. Finally, we impose a "floor" on our uncertainties, that is, we do not allow our quoted uncertainties to take on values smaller than appear realistic in view of our knowledge of the bubble chamber optics, etc.

There is a small difference in the track variables put out by the PANG and THRESH reconstruction programs. In addition to the usual two angles, PANG passes on the projected curvature of the track ($\propto(\cos\lambda/p)$ whereas THRESH passes on the reciprocal of the momentum ($\propto 1/p$). For most tracks, these variables are nearly equivalent, and there seems to be little reason to chose one over the other. A variable such as curvature is preferred over the momentum because there is reason to believe that for most tracks (tracks which do not stop the curvature is more nearly Gaussian distributed than momentum.

Although still in common use, the above PANG track reconstruction scheme has several disadvantages. For one thing, the curve fitted to the track is actually an expansion about a straight line. Table II indicates the performance of this simple procedure and points out its limitations in the case of tracks that bend through large angles. As chambers become larger and magnetic fields become greater, a more

suitable first approximation to the particle orbit is a helix (7). Tracks that turn through large angles also pose problems for the corresponding-point method of stereo reconstruction. Consequently the trend in more recent reconstruction programs is toward procedures that cope with both these problems by fitting a helix to sets of rays traced from each measured film point in each view through the optics into the chamber. For example in THRESH the reconstruction of tracks proceeds by the following stages: first test for poor measurements by fitting a circle through the measurements on each view, then find all the coefficients defining the equations of the light-rays intersecting the track and corresponding the measurements, then find a first approximation for the helix, without fitting, using a few of the reconstruction rays, and finally, find the best helix by a least-squares process using all the measurements in all views (up to 4 views can be measured).

An alternative but very closely related reconstruction method consists of projecting a helix in space onto the film and minimizing the deviations between the projected helix and the measured track points (9). This type of approach to the reconstruction problem provides a very straightforward method for translating measurement uncertainties at the film directly into uncertainties in the track variables.

1.3 Kinematic fitting.

Most track reconstruction programs are not concerned with the properties of the event as a whole, but rather with the data of each track separately. As a consequence, the estimates of momenta and angles of all the tracks at a vertex are generally not consistent with conservation of energy and momentum, for a given assumption as to the interaction taking place at that vertex. These conservation laws can impose up to four equations of constraint on the track variables at a vertex. (When all four constraints are used we speak of a "4 C fit," if one momentum is unmeasured (as in a V) we speak of "3 C," etc., down to "zero C," which is just a calculation and not a fit. For some examples, see Fig. 2.

A fitting program accomplishes two different results. 1. It spends most of its time laboriously trying to fit wrong hypotheses which eventually it rejects. 2. Given a correct hypothesis it usually finds a minimum χ^2 in a few iterations and writes out the new fitted variables for future use. The Alvarez program that does this fitting is called KICK. It adjusts track variables subject to two conditions. First, the energy and momentum balance must be preserved for the interaction assumed at a vertex, and second, track variables should be modified as little as possible. The second rather vaguely stated condition is expressed more precisely in terms of a least squares-test of the following sort:

$$\chi^2 = \sum_{i=1}^{N} \frac{(x_i - x_i^m)^2}{\sigma_i^2},$$

where N = number of measured track parameters for vertex,

x_i = adjusted value of ith track variable,

x_i^m = original measured value of ith track variable,

σ_i = uncertainty of ith track parameter, estimated on the basis of external errors.

The actual program involves a more generalized matrix expression that allows for correlations between track variables, but in the following discussion we simply ignore this. It should be pointed out that for simplicity and economy of computations, the measured variables are assumed to have Gaussian distributions about their true central values. Plural scattering, for example, results in a deviation from the assumed Gaussian form and contributes to unexpectedly large numbers of high χ^2, which are discussed in Section II, paragraph 2.2.

There are several ways in which one can minimize the χ^2 test function while preserving the conservation laws at the vertex. KICK employs the method of Lagrange multipliers. The conservation laws can be expressed as implicit constraint functions between the track variables:

$$F_J(x_1, \cdots x_N) = 0 \quad , \quad \text{for } J = 1 \cdots C.$$

where C is the number of constraints on the variables at the vertex. Then one can minimize the expression

$$\chi^2(x_1,\cdots x_N, a_1,\cdots a_c) = \sum_{i=1}^{N} \frac{(x_i - x_i^m)^2}{\sigma_i^2} + 2 \sum_{j=1}^{C} a_j F_j (x_1,\cdots x_N).$$

This is a very simple task if the F_j functions are assumed linear in the parameters x_i, for it involves solving only C simultaneous linear equations to evaluate the a parameters. Each x variable is obtained by substituting the a parameters into a simple linear expression containing only terms involving a. In practice, the F functions are not linear and it is necessary to iterate this procedure in order to obtain the correct coefficients for a linear expansion of each F in terms of the x parameters at the solution.

In addition, the coding has been extended to provide an overall fit to the more common two-vertex configurations such as the production-decay sequence of Σ^+ hyperons (both $\Sigma^\pm$ and also Σ^0). The less common multivertex fits can frequently be handled through a series of single-vertex fits in which each new fit successively uses the adjusted information from tracks connected to previously fitted vertices. This procedure has two disadvantage: 1. Only the last-fitted vertex incorporates all the experimental input; the earlier fitted vertices would have to be refitted in order to calculate best values and an overall χ^2, this is clumsy; 2. There are some multivertex events in which a single vertex taken alone is underdetermined, but the event as a whole is overdetermined. In such cases, a string of single-vertex fits may not be possible because an early vertex in the string is underdetermined. The CERN kinematics program, GRIND, written by R. Bock (10), is a more recent and general fitting code which overcomes this difficulty by fitting the event first at individual vertices and second (automatically) as a whole. This approach to the multivertex problem provides a well-defined χ^2 for the fitting hypothesis, as well as

the simultaneous best fit at every vertex of the event.

Even after a set of parameters that minimizes χ^2 has been established, there remains the question of the uniqueness of the minimum. For fits which are overdetermined by two or more constraints (i.e., $\geq$ 2C) we know of no problems with double minima; however for 1C fits there is an ever-present danger which can best be understood by considering a zero-constraint calculation, which is merely the solution to a quadratic equation with two roots. In the case of a 1C fit either of these 0C roots may form the basis for a mimimum, and if one of the variables entering in the 1C fit is poorly measured, the two minima may be poorly separated. This particular problem has been considered by Horace Taft, who has proposed that both minima be sought by starting the KICK search at each of the possible 0C solutions.

In structure, the kinematics program KICK is basically a collection of subroutines which are called upon by a group of short control programs ("event type" codes) to carry out the operations required to fit various kinds of events. The most important of these subroutines is GUTS, which carries out the actual fitting described in the previous paragraphs. Some of the other functions include input and output, transformation ("swimming," i.e. the transformation of variables (including error matrices) from one end of a track to the other, and preparation of tracks for the fitting process. Of course, the nature of the interactions assumed for each vertex and the actual sequence of fits attempted depends entirely on the experiment being analyzed and the track topology of the particular event. Each new experiment usually requires a new set of event type codes. Therefore a great deal of effort has gone into making the event type coding simple and short by including as much of the coding into the KICK subroutines as possible.

To eliminate writing and rereading an intermediate tape, PANG and KICK have been combined into one package (called PACKAGE) which contains 19,000 words of coding (excluding the event type coding). PACKAGE output currently runs about 2000 words/ event, but we are just incorporating another computer pass with a new program called WRING which manages to reduce the output to 600 words/ event by selecting only the "non-failing" hypotheses (i.e., the results of both successful overdetermined fits and of underdetermined hypotheses, such as the computation of a missing mass). WRING passes along the error matrices on fitted variables, and will be our primary source of fitted data.

1.4 Data Summary.

The next program, called EXAMIN, reads the PACKAGE/ WRING output and calculates for each event all the physically interesting variables that the physicist may want written onto a data-summary tape. These variables are such quantities as direction cosines and their errors, and invariant masses of groups of particles and their errors. Typically this adds up to 300 words/event. The CERN versions of WRING and EXAMIN are now running under the names of BAKE and SLICE.

The final major program is SUMX; in use both at CERN and Berkeley. It examines the data summary tapes (DST) and produces many sorts of displays. This particular program is entirely

independent of conventions as to the DST, and is available to anyone who would care to use it to summarize any sort of data. SUMX has a subroutine that permits one to easily specify sequences of logical tests for selecting events. It uses an oscilloscope to make scatter diagrams; its other outputs are printer tapes and occasionally, condensed data-summary tapes.

The scatter diagrams are used most often to make Dalitz plots. The most popular printer outputs are display histograms, ideograms, "resolution functions," two-dimensional histograms, and "ordered lists." In Section II we discuss some of the physics considerations involved in using each of these outputs.

1.5 Library programs.

Pencil-and-paper-type bookkeeping becomes impractical when the number of events processed exceeds a few hundred. Beyond this volume of events, a program designed to maintain an event catalogue becomes an important part of the data analysis scheme. The LINGO (11) program represents one approach to this library problem. LINGO operates in parallel with the data-analysis system, collecting information on any change in the state of analysis of the events. The basic tool of LINGO is the event catalog or master list containing the current status of every event in the experiment. Physically, the event catalogue is a magnetic tape containing information on as many as 100,000 events. Whenever necessary, the Master List is updated with new scanning information, measurement requests, modifications, or results. The master list is also available for producing listings, tallies, and other types of reports concerning the current status of the experiment.

1.6 The Quest System.

One unique analysis tool currently employed at Berkeley is the QUEST system. QUEST is a combination of hardware and programming designed to facilitate the analysis of small numbers of troublesome or unusual events that may not have been provided for in PACKAGE. The basic hardware consists of a

typewriter connected directly to an IBM 709 computer. A special modification of the PACKAGE program has been written which allows the QUEST operator to communicate the fitting procedure for a particular event to the computer through the QUEST typewriter.[2] Results from the fit are typed back to the QUEST operator within a few seconds after a fit to a vertex hypothesis has been specified. The operator may proceed with the analysis of the event, or on the basis of the information returned to him on the typewriter attempt to fit a different hypothesis.

The QUEST system may also be used in a semiautomatic mode. The sequence of operations carried out in the analysis of an individual event is saved in core. Then any further events requiring the same analysis pattern can be processed by having the QUEST program operate from the stored fitting sequence. If this "event type" is required for subsequent processing the stored fitting sequence can be punched out on cards and saved. A further feature is that the measurements used in the QUEST fits may be modified at the option of the QUEST operator. A track measurement beyond a specified point may be "chopped off" if the track is suspected of having a small-angle scatter or a collinear decay that is affecting the kinematic fit. An on-line Franckenstein has been added to the basic QUEST system, making it possible to remeasure one or more tracks that appear to be sources of trouble on the basis of attempts at fitting carried out at the typewriter. However, at Berkeley this mode of operation has been far less popular than the straight typewriter console mode which uses as input a magnetic tape containing previously measured events. Simple chores may be performed at the computer while QUEST is using the computer. Currently, the computer is used as a tape printer during QUEST operation. More ambitious computing tasks may be carried out during QUEST operation by interrupting QUEST with a standby program while the operator is pondering over his output. Figure 1 is an example of the dialogue between a QUEST operator and the computer.

2. ANALYSIS OF EXPERIMENTS

2.1 Dalitz Plots.

Many properties of three-body final states can be displayed by making a scatter plot of either

$$T_i \text{ vs } T_j \qquad \text{or} \qquad m_{ij}^2 \text{ vs } m_{jk}^2 ,$$

where T_i is the kinetic energy of particle i in the three-body center of mass and m_{ij}^2 is the invariant mass of the ij "diparticle," i.e.,

$$m_{ij}^2 = (E_i + E_j)^2 - (\underline{P}_i + \underline{P}_j)^2 .$$

It can be shown that unit area on such a plot ($dT_i dT_j$, dm_{ij}^2 dm_{jk}^2, etc.) is proportional to Lorentz-invariant phase space (12). Of the two variables, m^2 seems to be the most universally useful, because resonances or anomalies will show up at the same place in different experiments or in a single experiment with a large spread in beam momentum; such a situation is displayed in Fig. 3.

Occasionally, instead of being interested in the properties of two out of the three final-state particles (for which we have just said that m_j^2 is the best coordinate) one wishes to study the overall final state (for example when displaying decays of θ or η mesons). In this case it is wise to "normalize" the coordinates so as to make the envelopes for each event coincide as nearly as possible (13). Normalized Dalitz plots then exhibit clearly the behavior of matrix elements near the envelope, which represents collinear decays.

Note that a Dalitz plot contains no information about the beam direction, unless the data have been selected to correspond to a subset of production angles.

In concluding our discussion of three-body states we should warn that the normal population for β decay is not proportional to an element in Lorentz-invariant phase space ($dn_{L\cdot I} \propto d^3p_1 d^3p_2/E_1E_2E_3$), but instead follows old-fashioned "three-momentum space" ($dn_\beta \propto d^3p_1 d^3p_2$, see Ref. 14). Thus on a Dalitz plot β decay(14) appears to have a matrix element proportional to $E_1 E_2 E_3$.

Four-body final states--Triangle plots. --There is no way to represent four-body final states that is quite as satisfactory as a Dalitz plot, but one useful grouping is shown in Fig. 4. Figure 5 shows a "triangle plot" for such a pairing (15). The name comes from the fact that the boundary is a right triangle, as can be seen virtually by inspection. The density of Lorentz-invariant phase space inside the triangle is unfortunately no longer flat (12, 16), but is given in terms of the variables shown in Fig. 3 by

$$dn = \frac{4\pi^3}{M}\, p_{12}\, p_{34}\, dm_{12}\, dm_{34}\,.$$

Here $p_{12} = \frac{1}{2}|\underline{p}_1 - \underline{p}_2|$, $p_{34} = \frac{1}{2}|\underline{p}_3 - \underline{p}_4|$, and p is expressed in the overall center of mass, where $p = |\underline{p}_1 + \underline{p}_2| = |\underline{p}_3 + \underline{p}_4|$, and M is the invariant total mass.

2.2 Resolution Functions.

Before we can discuss resolution functions, we must define what we mean by a "histogram" and an "ideogram" and the difference between the two. Consider a set of numbers, m_i, each of which has an uncertainty δm_i. To plot a histogram one selects reasonable sized cells, Δm, and simply plots the population for each cell. To plot a Gaussian ideogram, one assigns to each event a probability described by a normalized Gaussian with central value m_i and standard deviation δm_i, and then one adds up all these probabilities. A useful rule of thumb is that the full-width Γ at half maximum of an ideogram tends to be about 4/3 the average δm.

In 3 we discuss why ideograms are much overused to display data, but here we point out that they are useful for calculating "resolution functions."

To illustrate the use of a resolution function, suppose that one sees a resonance with an apparent full width of 10 MeV. For each of the events in the peak suppose that the kinematics program has calculated the mass uncertainty δm_i, which may vary from a few MeV to tens of MeV. One then asks the question: if the true width of the resonance were zero, how wide would a histogram of the

resonance be merely because of these experimental errors? To answer this question one merely makes an ideogram of all the events, with the central value of each point set to the same arbitrary mass, but treating each point with its correct δm_i. That is a resolution function. If the resolution function is narrower than the observed width of the resonance, then the difference is probably due to a real physical width.

Note that the observed width of a resonance is most directly found from histograms, not ideograms. The equivalent ideogram is wider by a factor of about $\sqrt{2}$; because of this decreased resolution, ideograms are not even very useful for hunting for resonances.

It is known that the χ^2 distribution for the experiment under discussion is a little too broad by a factor a^2 (as it usually is -- see the discussion in 4), then in the absence of more detailed knowledge of the broadening, all calculated errors should be increased by a factor a before the resolution function is constructed.

2.3 Histograms and Ideograms.

We have described the difference between these two displays in 2.2. Here we want to discuss whether it is ever appropriate to use ideograms.

We feel that it is thoughtless and unwise ever to present data in form of an ideogram alone. But it is often interesting to present in one figure both a histogram and an ideogram of the same data.

Some objections to ideograms are:

1. They convey very little feeling for statistical fluctuations.
2. They do not permit the reader to combine the results of different experiments.
3. They are an insensitive way to display a resonance, since the peak will have a width greater than its true-plus-experimental width as displayed by a histogram (see 2.2).

The most useful application of an ideogram is to test statistical validity of a histogram peak that may or may not be a real resonance. If the questionable "spike" is real, then the ideogram should be only slightly wider than the spike; if the ideogram is too broad, this suggests that the spike is a fluctuation.

2.4 Chi-squared scale factors.

Most bubble chamber groups find that their χ^2 distributions for kinematically fitted events are too wide by a factor χ^2 of not more than two. This factor does not seem to depend in any simple way on "constraint class" (as defined in paragraph 1.3). Its meaning is that some or all of the uncertainties in track variables are underestimated by the stereo-reconstruction program. Part of this is to be expected, since real Coulomb scattering distributions have tails (due to plural scattering) which we fail to take into account. But most of this underestimate seems to arise from a host of poorly studied effects: turbulence, optical distortions, inexact optical constants in the reconstruction program, etc. All these small effects become increasingly important at higher momenta, where sagittae become relatively small.

We have tried to associate the large a^2 with some single track variable--curvature, dip, or azimuth--but have failed to establish a correlation. This test is easily made by looking at the distribution of the "normalized adjustments" or "stretches" written out by KICK [see Berge, Solmitz, and Taft, Rev. Sci. Instr. 32, 538, (1961), Sect. V]. If all variables are right[3] on the input, then after a fit their stretch distributions should be Gaussian with zero central value and unit width. However, if one single variable is underestimated (and the others are still right) one expects the stretch distributions for this variable to be wider than for the properly estimated ones. (This expectation does not apply for 1C fits, where all stretches are equal; see ref. (17). We find experimentally that usually all of the stretch quantities are too wide by about the same factor of a (the same a by whose square the χ^2 distribution is scaled). There are exceptions which

provide us with clues as to weaknesses in our data reduction techniques. For instance the stretch distributions for beam tracks, short tracks with few measured points, and tracks that stop are more irregular than most.

It seems to be general bubble chamber experience that if one scales χ^2 by the factor a^2, then the χ^2 distributions have almost their theoretical shapes, with not more than 5% to 20% too many events in a tail.[4] We also must admit that we have found it necessary to introduce lower bounds on the uncertainties calculated for angles (long tracks are assigned uncertainties which are too small to be consistent with our present knowledge of the optics). These "floors" are 1/4° in declination and 1/16° in azimuth.

Some typical values of a^2 for reactions produced in the 72-inch chamber by 1.5-BeV/c K^- are: a^2(1 constraint) = 1.76, a^2(2C) = 1.58, a^2(3C) = 1.71 for a sample of 5000 Λ decays or a^2(3C) = 2.0 for a sample of 1500 decays, a^2(4C) = 1.66 for a sample involving 1800 Λ decays or a^2(4C) = 1.76 for a sample involving 1500 K_1 decays.

What should one do about a^2? Ideally one takes the time to understand which errors are underestimated, and then corrects the equations that calculate these errors. Most groups have not done this, but are not quite willing to conceal the problem by increasing error estimates without good reason. Instead we merely scale χ^2 by a^2 before making statements about the confidence level of a fitted event. If we make resolution functions (see 2) we assume that all input errors are equally too small by a and guess further that all output errors are equally too small by a, so we multiply them all by a.

2.5 Distributions in mass vs distributions in mass squared.

In our discussion of Dalitz plots in 2.1, we have already pointed out that it is better to plot mass squared, m_{ij}^2, rather than mass m_{ij} because unit area is then proportional to the element of Lorentz-invariant phase space. In this paragraph we

we want to point out that a low-mass peak in a mass spectrum (e.g., the spike in missing mass corresponding to a π or a γ) shows up as a Gaussian-distributed peak if plotted in m^2, but is distorted if plotted in m (and of course if m^2 is negative the missing mass becomes imaginary). This situation is illustrated in Fig. 5, for which it is assumed that the distribution in m^2 is Gaussian. Then, since dm^2 is $2m\,dm$, the distribution in m must be skewed by a factor $1/m$. The magnitude of the skewing can be suggested by the shift of the peak m^* in the m distribution from its correct value. For a small shift, the peak m^* would be given by

$$m^* = m + \sigma^2 / 4m^3$$

where m = true value of particle mass (peak of m^2 distribution),

and σ = width of m^2 distribution [σ^2 has dimensions of $(\text{energy})^4$].

One is empirical: experimental histograms do resemble Fig. 6. But the real reason is illustrated in Fig. 7. Assume that the only appreciable measurement errors are those in momentum $\underline{p}_i$ ($i = 0, 1, 2$), and that each is Gaussian-distributed with a small fractional spread. Call the unbalance in energy (i.e., the missing energy) E, and the missing momentum $\underline{P}$; then the missing mass is written

$$\begin{aligned} m^2 &= E^2 - P^2 \\ &= (E_0 - E_1 - E_2)^2 - (\underline{p}_0 - \underline{p}_1 - \underline{p}_2)^2. \end{aligned}$$

If $m^2(p_i)$ were a linear function of the p_i then it too would be Gaussian distributed. Clearly it is not linear, but we can expand m^2 in a Taylor series about the true values of p_i; calling $\delta_i = p_i - p_i^{\text{true}}$, we have

$$m^2 = m^2_{\text{true}} + \sum_i \frac{\partial m^2}{\partial p_i}\,\delta_i + \frac{1}{2} \sum_{i,j} \frac{\partial m^2}{\partial p_i\,\partial p_j}\,\delta_i\,\delta_j + \cdots .$$

The reader can easily convince himself that the terms of order δ^2 squared and higher tend to be small, so that m^2 is to a good approximation linear in the p_i and hence approximately Gaussian, which is what we wished to show.

There is of course no point in discussing events with a small missing mass until one is sure that the event is not an "elastic" one from which no neutral particles escaped at all. To test this one could of course fit the event by using all elastic hypotheses, but this takes computer time. We have found it faster, at Berkeley, to have KICK calculate a quantity called χ^2(Un3)--the χ^2 test that there is no unbalance in vector momentum (3-momentum)(18). This χ^2 does not depend strongly on mass hypotheses, which may be wrong or ambiguous, and a single calculation may obviate more than one fruitless fit.

2.6 Monte Carlo Techniques.

At some stage in the development of a bubble chamber data-reduction system, it is necessary to seek out possible biases in the computations of the programs, and in general develop an understanding of the limitations and properties of the analysis system. Frequently, particular experiments have very special sources of bias, which must be examined. As an aid to such studies, it is useful to be able to generate large samples of event measurements that differ from one another in a manner consistent with Coulomb scattering and measurement uncertainty, but for which the correct mean values of the track parameters are known. The routine analysis of such a collection of events will reveal the behavior of the analysis system on a sample with known properties. A few projects suitable for study by a Monte Carlo approach are listed below.

Simulation of track measurements:

1. Checking of newly coded programs.
2. Adjustment of uncertainty parameters.
3. Estimate of biases in program computations and approximations.
4. Establishment of the realm of usefulness of a program.
5. Study of correlations between variables.
6. Study of the shape of track-variable distributions.

Simulation of event measurements:

7. Estimate of biases from kinematic fits to background events.

Simulation of experiments:

8. Analysis of the probability of erroneous conclusions due to statistical fluctuations.

2.7 Monte Carlo generation of track measurements, SIMULATE.

For Monte Carlo studies based on calculations at the early stages of the analysis system, it is sometimes necessary to generate samples of events which simulate actual track-point measurements as realistically as possible. The SIMULATE programs have been written to generate such samples of events. By feeding these artificial measurements into the analysis system, one can examine the distributions of parameter estimates at any stage of the analysis with a knowledge of what the correct estimates and distributions should be.

The first step in the simulation of a track measurement is the generation of a particle orbit in the bubble chamber. SIMULATE starts from a specified point in the chamber with a specified orientation, momentum, and mass and proceeds to generate(in the direction of either increasing or decreasing momentum) a track of specified length (unless the track comes to rest first, of course). The track is generated by adding a short segment to the existing track, re-establishing the momentum and magnetic field and modifying the direction to account for Coulomb scattering, then adding another segment; and so on until the track is complete. Points along the track are traced through the optics to their image points on the film in each of several views. Measurement uncertainties of the type present in the Franckensteins is applied to the film points to generate measured film points. Similarly, fiducial measurements are perturbed by an amount consistent with uncertainties in fiducial measurements. The whole event is put out in the standard format required by PACKAGE.

The Coulomb scattering or measurement uncertainty may be suppressed by zeroing appropriate parameters. Table II (in Sect. 1.2) includes examples of events

processed by PANG with both Coulomb scattering and measurement uncertainty suppressed.

2.8 Monte Carlo generation of events, FAKE.

The detailed simulation of events provided by SIMULATE is not usually required for estimating kinematical biases in the separation of competing fit hypotheses. For these cases, it is far simpler and faster to treat the problem by generating artificial input at a later stage in the analysis, for example KICK input. FAKE (3) is a Fortran Monte Carlo program that generates events in a bubble chamber according to prescription, and simulates the output of the PANG track-reconstruction program. To do this, FAKE generates events of a specified type according to a phase-space distribution, or to some other distribution that can be written down. In some cases, it is more convenient to use an actual sample of events to establish a correct distribution of events in the chamber (for studying the probability of fits to background events, for example). It places these events in a bubble chamber, takes into account secondary interactions, and calculates the errors that the stereo reconstruction program would have assigned to the measured quantities for these events. Then it modifies the measurable quantities in accordance with the errors. Finally, FAKE writes out this information in such a form that it can be used by the hypotheses-testing program KICK or PACKAGE.

The development of FAKE was principally motivated by the desire to study problems of misidentified events, the better to understand and identify the ambiguous events that occur in bubble chamber analysis. It can shed light on such problems as how often the reaction $\bar{p} + p \rightarrow \pi^+ + \pi^- + \pi^0$ simulates $\bar{p} + p \rightarrow \pi^+ + \pi^-$, how often as Σ^0 "FAKES" a Λ, or how often a leptonic Λ decay fits a two-body decay. Thus the FAKE program merits its name for two reasons: (a) it simulates PANG output, and (b) it is designed to study those cases in which one type of event is

faked by another.

Because FAKE operates on an event-by-event basis, it is able to produce data with the experimental resolution folded in much more realistically than can be done with other methods. Therefore it can be used to see what a given distribution in the center-of-mass system should look like in the laboratory system. FAKE also writes output tapes in the format of a data summary tape (one event per record). Although this output cannot be used to test hypothetical fits, it is very useful in the Monte Carlo generation of experiments for the purpose of designing the experiment itself, for calculating scanning efficiencies, or for other reasons.

One subroutine used in FAKE, namely GENPCM, has been isolated from the program and is available to generate events of n particles ($3 \leq n \leq 10$) distributed according to phase space. By using GENPCM, one can calculate with little programming the phase-space distribution of any quantity. Furthermore, one can modify the calculation to include a factor for any matrix element that can be written down.

2.9 Monte Carlo generation of experimental distributions, GAME.

There is another small Monte Carlo program (GAME) that has proven useful in evaluating experimental distributions (3). It generates many independent experimental distributions, according to any prescribed equation for a particular number of events, and plots these in histogram form. This can be used to help us to understand what statistical significance should be given to a particular deviation from the assumed distribution.

2.10 Minimizing Procedures.

There is always a variety of specialized problems requiring optimization of parameters. These optimizing problems range from measurement-analysis problems (such as fitting magnetic fields with empirical functions) to experiment-analysis problems [such as establishing phase shifts or scattering lengths, or fitting angular distributions, see, e.g., References (19) and (20)]. Two commonly used procedures for establishing optimum values are the maximum-likelihood method and the least-squares procedure Both these methods take the best parameter set as being the one which occurs at an extremum of a function. Therefore the problem can be reduced to one of finding a minimum of a general function of some number of parameters. (Maximum likelihood requires a maximum, but by changing the sign of the likelihood function, the problem can be converted to a minimization problem.)

There is a variety of procedures for finding the parameters at a minimum (21). These usually fall into two classes: those that repeatedly attempt to reach a minimum directly in one step (iteration procedure) and those which gradually approach a minimum through a series of steps, usually of decreasing size (stepping procedure). Both methods have their applications. The iteration schemes are particularly suitable for fairly straightforward problems in which it is easy to evaluate the first derivative (and perhaps the second derivative) with respect to all the parameters of the problem. For example, if both first and second derivatives are available, one can use Newton's method to solve the problem. In this case the function to be minimized can be approximated by

$$f(x_i) = \text{const} + \sum \frac{f_{ij}}{2} (x_i - x_i^0)(x_j - x_j^0),$$

where (x_i^0) represents the parameters at the minimum.

Then it is easy to show that the minimum of f is at

$$\vec{x}' = \vec{x} - \vec{\nabla} f \cdot (f'')^{-1},$$

where $\vec{\nabla} f$ is the gradient vector of f evaluated at $\vec{x}$, and f'' is the second derivative matrix evaluated at $\vec{x}$ (with components f_{ij}). This solution is exact if f is no more than quadratic in the parameters, but most problems require that the procedure be repeated, replacing $\vec{x}$ by $\vec{x}'$. Matrix inversion is a commonly available subroutine, and this procedure can be coded in a few FORTRAN commands.

Although iterative schemes are very suitable for most problems, there are those few cases where the iterative approach to a solution will lead merely to numerous frustrating and unsuccessful encounters with the computer. If the problem involves the parameters in some very complicated way and the nature of the function to be minimized is expected to be complex (multiple minima, unallowed regions for the parameters, etc.), then it may be more practical to use a stepping procedure to reach the minimum. For one thing, a complicated function may require numerical evaluation of the gradient. In an iterative procedure, the step depends on a knowledge of the first and second derivatives of the space and the value of the gradient, and a very large erroneous step can be introduced by a poor differencing calculation. With a stepping procedure, the damage is at worst one poor step. The stepping procedure also provides a mapping of the intermediate points between the starting position and final position. It is sometimes useful to know that no other minima lie along the line of descent between a particular starting position (possibly based on an old experiment) and the final value. The FORTRAN program MINFUN has recently been coded to seek a minimum according to the ravine stepping procedure (22). The MINFUN approach has proven helpful in several problems so far, but only further experience will determine the realm of usefulness of the program. The actual strategy used by MINFUN is best illustrated with a hypothetical function of two variables, f(x, y).

Figure 8 shows "contour lines" for the function [i.e., all (x, y) on a line have the same value for the function]. The hunting procedure involves in sequence two different sorts of steps, an "overstep" to a point O and a "sidestep" to S, followed by calculation of a new minimum along the line OS; then the cycle repeats with a new overstep to point O' from the last minimum and through the new minimum. In more detail, the search starts at point M, where the starting direction is taken as being along the gradient. A step of fixed size is taken along this direction to a "reconnaisance" point O, where the function and its gradient are determined. A step is taken transverse to the line MO from the point O to point S. At point S the function is evaluated. From the information available at points O and S, a minimum is predicted at point M' along line OS by assuming the function varies quadratically along the line OS. The function is calculated at point M' to verify the minimum at that point. (In case M' is not a minimum relative to O or S, a smaller sidestep is taken.) To complete the cycle, a step is now taken to a point O' along the line MM', and the operation repeats as described at point O. As described, this procedure does not stop at the minimum, but continues right on along the "ravine" in the function. This is a useful mode of operation, for it allows a mapping of those sets of parameters which give rise to values of f near the minimum. This procedure tracks a ravine until about the spot where the minimum radius of the "contour lines" exceeds the step size, after which the search usually doubles back on itself. The actual position of the minimum is determined by altering the above procedure to the extent of reducing the step size and reversing direction each time steps lead to increased values of f.

3. ECONOMICS

3.1 Manpower and Machines.

An operation such as the one discussed so far involves large groups of people; no discussion of conventional data analysis is complete without some comments on numbers of men and machines. The Alvarez group (including visitors) numbers about 20 in each of the categories – Ph. D, graduate students, and computing staff. This does not include personnel primarily concerned with building and operating bubble chambers and advanced data-analysis apparatus. To process 72-inch chamber data there are in addition about 60 full-time equivalent scanning and measuring technicians, and 20 maintenance technicians. We have four Franckensteins to measure 72-inch film, and 12 scanning projectors. During the first half of 1963 the four Franckensteins measured about 6 events/hour, and each operated 120 hours per week, giving an annual production of 140,000 events/year. To process these 140,000 events we use 70 hours/week of 7090 time, of which 50 hours are taken up by the data-processing programs listed at the top of Table III,[5] and 20 hours are devoted to physics and Monte Carlo programs and program development. QUEST and SMP (see 4.2) share a 709 contributed almost free by IBM to help us develop on-line systems.

3.2 Costs.

Our principal costs are itemized in Table III. They include salaries, overhead, maintenance, and depreciation over ten years (23). Scanning, measuring, and event processing (items 3 through 5) deserve special comments. In actual practice, we find that, for one reason or another, film is usually scanned at least twice. Similarly, only about half of the event measurements find their way into the final published physics. (The unused half is made up of event measurements that failed and had to be remeasured, or events discarded for lying outside of a standard acceptance region in the bubble chamber or are discarded simply

because they fit no interesting hypothesis.) As a result, the cost estimates for these items can realistically be multiplied by a factor of at least two for our present mode of operation. The computer costs in Table III do not include special calculations concerned with the experiment as a whole. A more detailed breakdown of the computations is available in Table IV.

In Table IV we compare the actual use of computer time with the theoretical minimum times taken from Table I, which would apply if each event were processed only once and if there were almost no activity (LINGO, SUMX, etc.) on an experiment until all events were processed. This would, of course, be unreasonable. For example, we write the PACKAGE event types as simply as possible, ignoring the possibility of rare decay modes, and later reprocess all those events that fail to fit simple hypotheses, or give other clues of being interesting. The reprocessed events go through a much more complex version of PACKAGE, EXAMIN, etc.

Our logging of 7090 time is unreliable (a run through the whole sequence of programs may well get charged to the first program) but we have tried to reconstruct typical 7090 times for one experiment (K72) which was being processed in the first half of 1963. As we mention in footnote a. of Table IV, it is really nonsense to calculate "7090 sec/event," but we did it nevertheless to get some way to make a comparison with Table I. Rather than being linear in the number of events processed per month, many entries depend more closely on the number per experiment, and increase sharply with the number of physicists involved in the experiment, particularly if some of them have impatient personalities.

4. AUTOMATIC MEASURING AND SCANNING

A. Automatic Measuring - "am"

4.1 Definitions

Digital computers have been used for many years in the analysis of bubble chamber pictures, but only in the last few years has their performance-to-price ratio improved so much that it became economical to try to use them to assist in the measuring and even in the scanning of these pictures. In this section we discuss three automatic measuring (am) systems, which have come into operation during 1963, then we discuss two automatic scanning and measuring (asm) systems, which will be operating on an experimental basis in 1964.

First, however, we have better explain what we mean by the terms am and asm. Then we shall describe the systems, and finally with Table V we shall compare them and make some general comments.

The words "automatic scanning" are fairly descriptive; however, "automatic measuring" (am) is really only a name for the process of computer-assisted measurement, which we shall illustrate with an example. The real examples of am described below are the SMP, the spiral reader, and the FSD (operated in its am mode); for simplicity, though, we shall illustrate am with a device that does not exist, an am Franckenstein. Such a Franckenstein would have no track-following servo, but would instead have means of digitizing all bubbles on the projected image, within an "aperture" extending a few mm on either side of the conventional cross hairs. To measure, the operator would move the cross hairs along the general vicinity of the track image, moving as fast as he could while still being able to keep the track within the aperture. The area along the track, one aperture wide, is called a "road," and the first half of automatic measuring is to collect all the data inside a road and store it in the memory of a computer. The second half of am is accomplished by a "filter" program, which selects groups of 10 to 20 bubbles

and makes histograms of their positions across the road. By so doing it can filter track elements from background or from one another; it then links track elements into tracks. Next it calculates the coordinates of "averaged points" on each track and writes them out on magnetic tape in a format similar to Franckenstein output, suitable for conventional analysis programs.

It turns out that to filter one view of a typical track takes 1/10 to 1/4 sec on a 7094, and that it is now more economical to dispense with track-following servos and rely on filter programs. A measurer can make a road several times as fast as he can accurately follow a track with a servoed stage. In addition one gets bubble density measurements as a free by-product.

As mentioned above, there are already three examples of am devices. These systems have been described in References 1 and 2, so we now give only a brief survey of each.

B. Three Automatic Measuring Systems

4.2 The Scanning and Measuring Projector--SMP.

This device (24) is cheap enough ($32,000, produced at Berkeley) that a single laboratory can purchase several and use them for simultaneous scanning and measuring; this eliminates annoying "handover" problems. All the SMP's are serviced simultaneously by a single computer. The computer may be carrying on functions not related to the SMP systems, (for example, general purpose computing or offline printing) depending on the capacity of the computer and the number of measuring tables to be serviced. Each SMP table is similar to a Franckenstein to the extent that a human being guides the device during measurements. The SMP measuring table consists of a straightforward optical and film-handling system which projects an image down onto a horizontal white screen. The machine resembles a conventional overhead-illuminated scanning table with two exceptions. First, located near each

SMP table, there is a typewriter that provides two-way communications between the SMP operator and the computer program. Second, the viewing screen is actually made up of movable white Mylar sheets which allow a 0.6-cm measuring aperture in the screen to be positioned anywhere on the projected bubble chamber image. Operationally, the SMP operator scans the film in a conventional manner, recording any required scanning information via the typewriter onto magnetic tape. When an event is found that is to be measured, the small movable aperture in the viewing screen is moved alongtracks or fiducial lines that are to be encoded, and the measurements are sent directly into the computer. The computer guides the operator through the measuring procedure by means of brief comments on the typewriter, and automatically performs some mechanical operations, such as switching views. The computer is able to detect some typing and measuring errors, and respond with corrective instructions to the operator. Immediate correction of errors results in a substantial time saving by eliminating the film handling for remeasurement later.

Mechanically and electronically an SMP table is simpler than a Franckenstein because the SMP does not rely on digitized microscope stages or a high-precision servo system to achieve its accuracy. The measurement precision of the SMP is attained by making measurements relative to an array of precisely placed bench marks which are contact-printed onto a glass photographic plate the size of the measuring table. The plate is opaque except for 20-mil clear spots ("bench marks") located each centimeter in X and Y. Coordinates along a track are measured with respect to nearby bench marks by displacing a track segment a known distance through a rotating periscope (rotating at 1200 rpm) that can be moved about in the image plane of the SMP table (see Fig. 9). As the displaced track segment sweeps over any bench mark, the periscope orientation is read off a magnetic recording on the rotating drum in which the periscope is mounted. This information is sent directly

to the computer along with information to identify the bench mark involved. The computer can reconstruct the track point by subtracting the periscope displacement of the track from the precisely known position of the bench mark. The SMP's presently in use at Berkeley digitize approximately eight points per centimeter on the projected image. Each point is digitized to a precision of 80 microns on the SMP measuring table, which is equivalent to about 5 μ on the film. Because so many points are generated along a track, the points are averaged in sets of ten to bring the number down to about that produced on a Franckenstein (with an uncertainty for the averaged points of less than 2 microns). Digitizations may occur for any part of the image that passes through the 0.6-cm periscope aperture, therefore one of the tasks of the computer is to filter out background bubbles or scratches that may be recorded along with the desired tracks. The digitization of a track point occurs only when a bubble of the track is swept across a bench mark by the moving periscope. If the bubble is absent (a gap in the track) the missing digitization provides information about the bubble density of the track. The high density of digitizations along a track makes such estimates of bubble density statistically meaningful.

4.3 The Spiral Reader.

One way of reducing the event-measurement time is to attempt to digitize all tracks radiating from a vertex in one operation. At Berkeley, the spiral reader has been developed for just this purpose (2, 25). Track points are recorded in a polar coordinate system, where the vertex of the event being measured is located at the pole. The image of the event is projected onto a radial slit which rotates about the pole, sampling all tracks radiating from the vertex. The radial position of the slit can be varied out to a distance of about 5 inches (equivalent to 1 in. on film or 15 in. in the 72-inch chamber). As the slit spirals out from the pole, the radius and azimuth of the slit are recorded at those positions where a track segment

passes over the slit, producing a drop in the light incident on a photomultiplier. A group of these polar coordinats is accumulated into a buffer memory and then transcribed to magnetic tape. In addition to the track points, some nontrack background is recorded. Here again, computers are well suited to rejecting the background. The Spiral Reader output tape is processed by the FILTER program, which filters out the background and produces a tape suitable for processing by the standard analysis programs (PACKAGE, etc.).

4.4 The Flying-Spot Digitizer-FSD.

The flying-spot digitizer is known throughout most of the world as the Hough-Powell Device (HPD) after its developers (1, 26). However, at Lawrence Radiation Laboratory the overall system has been christened FSD, which name we shall use, with apologies, because of its descriptive value.

There are two ways that FSD can be used--Phase I, -am, which has just begun production measurement, is the automatic measuring mode in which a human decides where the FSD should measure. Phase II, -asm -- described in 4.6 -- is fully automatic.

The operation of FSD (am) has been extensively described (1) elsewhere. It is a two-step process. The first step is the usual scanning operation, except that a few "road-making" points are digitized along tracks that are to be precisely measured later. The digitizing at the scanning table is done with rather simple low-precision digitizers with a least count of 120 μ on the projected image. After road-making points have been accumulated for a large number of events on a roll of film, the film is loaded on the FSD and each event that has been prescanned is automatically digitized with 1 μ precision by a flying optical spot capable of systematically scanning the film in a pattern resembling an ordinary TV raster. The Cartesian coordinates of any bubble intercepted by the scan spot (as detected by a photomultiplier) are transmitted to the computer to be processed while the scan proceeds. The scan spot is generated by passing light through a rapidly rotating

disk with nearly radial slits, then through a stationary slit and optics which image the spot on the film (see Fig. 10). This gives a rapid line scan with a 20-μ spot size (smaller than a bubble on the film). A portion of the light for the line scan is imaged on a grating so that the position of the spot can be determined by counting grating lines as the scan proceeds across the line. The raster is produced by uniformly moving the microscope stage (which carries the film) perpendicular to the line scan. Scan lines are separated by about 2 bubble diameters.

There are provisions for a special scan raster at 90 degrees to the normal raster. This flexibility assures good sharp track pulses for tracks at any orientation on the film. The FSD scan raster is fine enough to give an estimate of bubble density on the basis of the number of gaps in the tracks. Attempts to use FSD as an automatic scanning and measuring system are described in 4.6.

C. Automatic Scanning – "asm"

4.5 Automatic Scanning and Measuring.

There are now three major projects involving pattern-recognition programs for general-purpose computers coupled to special-purpose hardware, the whole system aimed at automatically scanning bubble chamber film. Since "pattern recognition" is such a general and difficult field, we shall use the more precise and less presumptuous name "automatic scanning." This problem is considerably harder than that of automatic measuring, which has just been realized in 1963; nevertheless, several complete schemes have now been outlined, and we guess that in a few years millions of triads will be scanned and measured automatically each year.

Actually, for two different reasons, all the present efforts described below are aimed at doing automatic scanning plus measuring (asm).

1. Present-day computers compete rather badly with humans doing pattern recognition, but they compete much better doing tallies and measurements. Therefore

a system that can scan and make coarse roads should certainly take advantage of the solved technology of automatic measurement.

2. Automatic scanning involves some annoying problems of matching vertices and tracks in three stereo views. The more precise the digitization, the easier is the logical problem of disentangling close and confusing vertices and tracks.

The three major assaults on asm are based on the hardware of FSD, PEPR, and Illiac III. The first two will be running on an experimental basis during 1964, and are summarized below. Illiac III is a less immediate, more general project which has been adequately described by McCormick (27), and is not taken up further here.

4.6 FSD (asm mode).

It was of course originally conceived that FSD would some day run as an asm system. This requires no hardware change; instead it envisions replacing the eight digitized scan tables and their personnel with one or two additional "shifts"** of 7094 time.

In 1961 Pasta, Marr, and Rabinowitz (PMR) began to work on a 7090 program (28) designed to sort data from the FSD input buffer as fast as it comes in (about 10,000 to 20,000 coordinates per sec). The program (which we call PMR) defines track banks and predicts where the next bubble should be found. When a new digitization comes in it is promptly compared with this prediction. If it checks, it is stored in an existing bank; if not, a new track segment is initiated.

Howard S. White (29) at Lawrence Radiation Laboratory is also working on a PMR program which he calls "DAPR" (Digital Automatic Pattern Recognition). He estimates that DAPR running on a 7094 can process 18,000 digitizations/sec, which is just the speed of the FSD at LRL. He finds that a typical scan of a single view of the Alvarez 72-inch hydrogen chamber yields about 72,000 digitizations;

so this scan takes 4 sec of DAPR time. We must then add about 50% in time for the "orthogonal scan", so that a view takes about 6 sec., and a triad takes 18 sec.

The output of PMR/DAPR will be a "single-view data tape" containing a few hundred computer words per view, mainly about 10 average points per track view, except for those tracks which pass through the chamber without interacting. The single-view tapes from DAPR and PEPR will be similar, and subsequent processing will be almost identical (30). This subsequent processing by programs called TRIAD and SCAN is discussed under PEPR, below.

4.7 "Precision Encoding and Pattern-Recognizing Oscilloscope"-PEPR.

This approach combines both digital and analog techniques into a system designed to automatically scan and measure bubble chamber film (31). The idea was conceived by Pless at MIT and all the hardware is being built there; Yale and Lawrence Radiation Laboratory have contributed most of the computer programming. In the PEPR system, a random access "spot" on a cathode ray tube is imaged onto the film under the direction of a small special-purpose computer. The "spot" itself has a variable shape ranging from a spot (25 μ diam) to a line with an aspect ratio of 80 (25 μ by 2 mm) which can have any orientation. Very briefly, PEPR consists of three units: about $100,000 worth of nondigital hardware associated with the precision cathode ray tube, optics and track-element detector, a grating system, and a film transport. This hardware is controlled by $100,000 worth of special-purpose digital hardware called the "controller." The controller is on line to a small general-purpose computer called PDP-1, which costs about $200,000. A considerable part of this apparatus is now working.

The orientable line is particularly suitable for recognizing track patterns. The flexibility of this scheme allows a three-phase attack on the scanning-measuring problem.

1. An overall area scan of the entire film can be carried out by using scans with a 2-mm "slit" (electron beam) of different orientations. The film is divided up into many 2-mm-square cells and the position and orientation of any track elements detected in these cells are fed into the computer memory. The "slit" direction is good to about 1 degree, and the position to 1 part in 4000 of the face of the scope. This procedure establishes a bank of data in core for each track.

2. The next phase is the track-following technique. The track (or track segment) in each track bank is followed in both directions until it ends or connects to other tracks, which can also be followed.

3. Finally, once interesting tracks are identified, the point spot is used to count bubbles and precision-encode coordinates.

It should be pointed out that this three-phase strategy is almost identical with that now being programmed for Illiac III (27), except that the scan of the 2 mm square window uses a digital rather than an analog processor.

The size and orientation of the PEPR "slit"--i.e., line segment generated on the face of the cathode ray tube--are controlled by adjustment of currents in a "diquarupole" focusing magnet, which produces an effect on the electron beam in the cathode ray tube which is analogous to the action on light of an orientable cylindrical lens.[6] Precision encoding is done using a point spot with beam splitters arranged so that a portion of the scanning-spot light is focused on a pair of "picket fence" gratings. These gratings consist of 25-μ dark "slats" separated by 25-μ open gaps. The two gratings are at right angles to each other; let us call one of them the x grating, the other the y. To digitize a bubble, the spot is servoed along one of the slats, y, and moved in the x direction. The x position is then counted with the same scaler and interpolation counter circuits used in the FSD device. As the spot crosses a bubble its x and y coordinates are stored in a register in the controller. As in all of these systems, bubble density information is available.

One PEPR should scan about a million triads a year, which is the same as

the estimate for one FSD. The main difference between the two is that whereas the hardware costs for FSD (asm) (i.e., without digitized scan tables) are probably less than costs for PEPR, FSD (asm) requires 2 to 3 shifts of 7094 time before it can produce a single-view data tape; PEPR requires none.

The single-view data tapes from FSD or PEPR will be read by a 7094 program called TRIAD, which will match vertices and tracks in all three views, and write a primary data tape. It is planned that this primary data tape will then be read many different times by another 7094 program called SCAN. SCAN will have processing routines easily called by a control subprogram or "event-type program." The event type will set forth scanning criteria, so that SCAN will scan the primary data in much the same way as a human now scans a film for an event of interest. SCAN's output will look like ordinary Franckenstein output, ready to be read by conventional analysis programs.

D. Comparison of Automatic Systems

4.8 Discussion of Table V.

To conclude this section, we summarize some of the important parameters of current systems in Table V. To construct this table we have taken a hypothetical large bubble chamber output of a million triads per year, and we have assumed that in this million triads there are a million interesting events. This ratio of measurements per triad is several times as high as that currently found for Franckenstein systems, but of course with automatic measuring, and particularly with automatic scanning and measuring, the difficulty of measuring is much decreased, and one will tend to measure more of the common types of events. It has been assumed that all the scanning and measuring tables are operated three shifts (120 hours/week); thus the number of salaries involved for Franckensteins is 99, for SMP 36, and for FSD (am) 24 (plus one operator per FSD shift). To process a million triads

PEPR has to work around the clock (one operator for each of the four shifts--which include week ends), and FSD (either mode) gets through in three shifts (again with one operator per shift).

Table V is divided horizontally into Franckenstein systems (for comparison with what lies below), systems that do automatic measuring only (am), and systems that do both automatic scanning and measuring (asm). The first point shown by Table V is that although individual Franckensteins are still productively measuring 30 to 40 thousand events per year, a troop of 30 Franckensteins is no longer the most economical way to measure a million events.

Next we come to the automatic measuring systems, all three of which have been doing experimental physics for only a matter of weeks. Given this fluid situation our estimates are surely not good to better than ± 50%, and accordingly it is hard to find any decisive difference in the cost of their operations. Note, however, that the spiral reader is most competitive for single-vertex events; its measuring rate decreases about 15% for each additional vertex, independent of the number of tracks at each vertex. In organization, there is a significant difference between SMP and FSD (am). It takes about the same amount of time and money to coarse-digitize an event for FSD as to measure it on SMP, but the SMP event is then ready to go into conventional analysis programs; moreover, so many checks have been performed that it is most unlikely that the SMP event will fail in the subsequent stereo reconstruction or kinematics programs. The price one pays for this is the need for an on-line computer. It would appear that five SMP's on line to a PDP-1 computer[7] is more satisfactory than five FSD scan tables and an FSD. A minimum configuration for an SMP system might consist of three SMP's attached to about a $230K computer. The computer could be used for SMP measurements during some shifts, and for physics analysis during others. Conditions vary from laboratory to laboratory; for example there are laboratories which do

not use their computers full time and a group of SMP s could make measurements during the times the computer would otherwise be idle. For a very small laboratory it seems more satisfactory to have on FSD scan table communicating via the mails to a distant FSD. In the absence of much operating experience so far it is hard to say where to draw the line between these examples. A vigorous defense of FSD vs SMP has been presented by P. V. C. Hough (32).

Next we come to some even more difficult comparisons between automatic scanning and measuring equipment that is not yet even working. PEPR (at $400K and no salaries except for maintenance and one operator per shift) will, if it performs as advertised, be the cheapest system in the whole of Table V. FSD (asm) involves slightly less initial hardware cost, but requires two to three shifts of 7094 time. The cost of this much computer time varies greatly from one installation to another, but probably averages $500,000 per year on today's computers. Since the days of the IBM 704 or 709, however, the cost of a computation has been decreasing about 50% each year, and this trend will probably continue. Hence in a few years this $500,000 computer bill may have dropped to $100,000 or $200,000, which is hardly a decisive expense, being comparable to the annual cost of purchasing and processing the film for our hypothetical million triads. On the other hand, half of the cost of PEPR is a smaller computer, and these also will get cheaper. We conclude that cost of operation cannot easily force a decision between FSD and PEPR. Morever as experience is acquired with both systems, they will each doubtless be quickly modified; the asm system of 1966 will probably contain the more satisfactory elements of both--a larger on-line computer than PEPR has, and better film random access than FSD has.

4.9 Photographic Memories.

The major obstacle to large-scale analysis of bubble chamber film has until recently been the measurement operation. Buth with automatic measuring, data rates will rise and it may be appropriate to look ahead to the immediate complications that will ensue as a consequence of a greater film-measuring capacity. An already formidable problem is the storage and retrieval of the data (both by humans looking for lost tape and by machines trying to read the tapes). For example, consider the amount of information that must be saved at the end of the analysis of each event. Our PACKAGE output can be condensed to 600 words per event, but for a million-event-per-year analysis system, this represents more than 1/3 million feet of standard 800-bit-per-inch magnetic tape (157 reels of tape). Just to read this much tape requires about 10 hours. The direct output of the PEPR or FSD alone would require at least twice this much storage. In addition to the PACKAGE input and output storage, there are the library master lists, and data summaries which are updated and summarized frequently.

Magnetic tape systems will undoubtedly be improved in the future, however, an alternative to the data-storage problem is the photographic memory (33). By exposing spots on a photographic plate or film, it is possible to store much more data in a form which is more quickly accessed by the computer. For example, using a cathode ray tube and 35-mm film strip in an arrangement similar to that described in PEPR, it should be possible to achieve a reduction in length to about 1/600 of an equivalent standard magnetic tape, and a reduction of read time by a factor of 10.

5. ACKNOWLEDGMENTS

We want to thank L. W. Alvarez and many people in his group for their help and comments. In particular we appreciate the suggestions of Margaret H. Alston, J. Peter Berge, Reinhardt Budde, Robert J. Harvey, Jack Leitner, Charlotte E. Mauk, Lucien Montanet, John H. Munson, Barrie Pardoe, Frank T. Solmitz, Howard S. White, and Stanley G. Wojcicki.

Table I. Alvarez Group programs.
(Further data on running times are given in Table IV.)

Program	Function	Type of coding	Approximate running time in 7090[a] (sec)	Approximate number of commands and storage	Average Words/event[b] Events/tape
PANAL	Check and format, sort, merge, select	9AP[c]	3.0/event[g]	15,000 17,000	250 14,000
PANG	Track reconstruction	9AP	0.2/track	8,000 2,000	see PACKAGE
KICK	Kinematic fit	9AP	1.0/vertex	11,000 5,000	
PACKAGE	Combined PANG and KICK	9AP	See above (typically 6.0)	19,000 7,000	2,000 1,200
EPC	Prints PACKAGE output	FORTRAN	3.0/event	11,000 16,000	Printer tape
EXAMINE	Analysis system for KICK output	FORTRAN	2/event	5,000[e] 19,000	30 - 1000 3K to 10K
SUMX	Experiment summarizing routines	FORTRAN	see footnote f	14,000 11,000	Printer tape
LINGO	Library system	9AP	3/event	20,000 12,000	40 100,000
	Subtotal (PANAL through LINGO)		~12 sec/event		
QUEST	Processor for unusual events	9AP	See PACKAGE	21,000 9,000	---
SIMULATE	Monte Carlo measurement generator	FORTRAN	1/track	10,000 8,000	---
FAKE	Monte Carlo event generator	FORTRAN	3/event	16,000 3,000	see PACKAGE or EXAMIN
MINFUN	Stepping minimizer	FORTRAN	?[d]	9,000[e] 5,000	---

UCRL-10812

Footnotes for Table I.

[a]For further details on running times for an actual experiment, see Table IV.

[b]We have taken 2000 ft of tape written at 800 characters per inch. This is 3.2 million 36-bit words.

[c]LC9AP is a machine-language assembler similar to FAP. Most of our gap programs are being converted to FAP.

[d]The time depends strongly on the particular job being done.

[e]This program makes use of FORTRAN programming contributed by the program user. The space estimate does not include the user's program.

[f]Normally many displays are generated during one pass through a DST tape, because SUMX is input-limited. A time estimate can be arrived at for a fairly typical run on 2500 events in which 125 displays (one-and two-dimensional histograms and a few CRT scatter plots) were generated with six tape passes in 7.6 minutes.

[g]This program is also used to merge and order measurement tapes. This accounts for the relatively long time estimate for PANAL.

Table II. Systematic errors in PANG fits. The input is in the form of track points, generated by the program SIMULATE, for pions in the 72-inch hydrogen bubble chamber with a uniform 17.9-kG magnetic field. Energy loss was taken into account, but not Coulomb nor measurement uncertainties.

	Momentum at beginning (MeV/c)	Length (cm)	Azimuth at beginning (deg)	Azimuth at end (deg)	Declination (deg)
Input	200.0	25.00	00.00	39.32	0.00
PANG Fit	200.1	24.98	00.03	39.30	0.00
Input	200.0	50.00	00.00	80.59	0.00
PANG Fit	201.3	49.59	00.78	79.57	0.00
Input	500.0	83.00	00.00	52.13	30.00
PANG Fit	500.2	82.84	00.09	51.99	30.09
Input	500.0	41.00	00.00	25.47	60.00
PANG Fit	500.0	40.99	00.00	25.47	60.00

Table III. Itemized costs of bubble chamber experiments.

	Operation	Unit	Approximate time	Unit cost ($)
1.	Accelerator operation		No estimate	
2.	Bubble chamber operation through processing of film	1 exposure ("triad")		1.20
3.	Scanning of film	1 triad	1 min	0.10
4.	Measuring of film	1 event	10 min	2.00
5.	Computer analysis of film measurement	1 event	12 to 60 sec (IBM 7090)	~1.00

Table IV. 7090 Running Times used by PANAL-through-LINGO for a typical experiment involving 50,000 events being measured at a rate of 60,000 events/year.

Program	Hours per month	7090 seconds per event measured: via hours per month[a]	7090 seconds per event measured: from Table I
PANAL SELECT	8	6	3
PACKAGE	27	19	6
EPC	2[b]	1.4	3
EXAMIN SUMX	17	12	2
LINGO	35	25	3
Miscellaneous	8	-	-
Total	~100	60	12

[a] During the typical month in 1963 for which this table applies, 5000 new events were measured. However the events processed were only partly new events. For example, the times taken by SUMX and LINGO were mainly spent reading through the 50,000 earlier measurements. Nevertheless, to have a comparison with Table I we have calculated "seconds/event measured" merely by dividing "hours/month" by 5000 events/month, and of course multiplying by 3600 sec/hour.

[b] PACKAGE output of most events is not printed.

Table V. Systems to scan a million triads, and measure a million events, each year. The assumptions behind this table are set forth in References 25 and 23 .

System	Number of measuring machines	Number of scan machines	System purchase cost ($K)	Computing Shifts (7094)		Digitizations per cm on film [f] (μ)	Slit or spot size on film	Typical least count on film
				Measurement	Analysis			
FRANCKENSTEIN	30($100K ea)[a]	3[m]($15K ea)[i]	3045	0	1 - 3[e]	10	5×300	1 - 2.5 μ
SMP (am)	12($32K ea)		380	1/6 of 3[h]		100	35 (spot)	$\sim 5\mu/\sqrt{n}$[k]
SPIRAL READER (am)	6[c]	3[m]($15K ea)	550	1.3[d]		15-30	10×700	~5μ
FSD (am)	1(250K)[l]	8[m](40K)[l]	570	1/3 of 3		170	23(spot)	$1\mu/\sqrt{n}$[k]
FSD (asm)	Tandem ($375K)[l]	0[b]	375	2 - 3[n]		170	23(spot)	$\sim 1\mu/\sqrt{n}$[k]
PEPR (asm)	1($400K)	0[b]	400	1/2[j]		100	25×(25μ up to 2 mm)	$\sim 5\mu/\sqrt{n}$[k]

[a] $100 K is an average American price, and includes track following; however, SOM (Paris) sells for $50 K a measuring machine without track following but with electronics and a CRT display of the signal from the slit.

[b] This system does not require scanning machine; however, it is certain that humans would occasionally want to look at the film. Therefore a few conventional scanning tables would be needed.

[c] Assuming one-vertex events.

[d] This estimate is for a program that is not yet optimized.

[e] One shift would be a bare minimum. Extrapolation of our present procedures would predict six shifts; perhaps three is a reasonable compromise.

[f] i.e., digitizations per cm of a densely ionizing track, projected (if necessary) back to film.

[g] P. G. Davey, Lawrence Radiation Laboratory, UCID-1891, 1963 (unpublished).

(Footnotes for Table V. (Continued)

[h] The notation "1/6 of 3" signified that 1/6 of the computing capacity of a 7094 is required for three shifts. For example, SMP's are assumed to operate three shifts (120 hour/wk) of real time so one must either choose a computer appropriately slower than a 7094 or share time. Time sharing implies either using a moderate computer like a 7044 for simple time shared jobs like printing or implies true multiprogramming on a large computer with a disc file. The SMP computing load is calculated on the basis of 2 sec 7094 time (30 sec 709) for the executive program plus filtering, and does not include PANG or "Economy KICK."

[i] The scanning projector manufactured by SOM, Paris, sells for $9000.

[j] Computer programs call TRIAD and SCAN will combine data from three views, make data libraries, and scan them for events of interest.

[k] Whereas Franckenstein and the Spiral Reader digitize the position of a slit which averages over several bubbles, the other automatic measuring devices digitize individual bubbles. Groups of about 10 of these bubbles are then averaged. For an infinite number of bubble $\sigma^2_{av} = 1/12\ \sigma^2_1$; for 10 bubbles, $\sigma^2_{av} \sim 1/10\ \sigma^2_1$.

[l] Lawrence Radiation Laboratory production costs as estimated by Jack V. Franck and Howard S. White; B. Powell quotes the CERN FSD cost as $ 90 K, and the cost of the economy model CERN FSD (am) scan tables as $13K.

[m] In actual practise additional conventional scanning tables are required. As an example, the present ratio of scanning tables/ measuring tables in the Alvarez group is 3/1. There are two reasons for these extra tables. 1. In the last year we measured only one event/10 frames scanned, as contrasted with one event per frame as assumed in this Table. 2. We tend to rescan each experiment about one extra time.

[n] Howard S. White, (Lawrence Radiation Laboratory), private communication.

FOOTNOTES

* Written under the auspices of the U. S. Atomic Energy Commission.

1 Our terminology is as follows. A vertex stands for the point in space where an incoming particle either reacts or decays, producing one or more outgoing particles. An event is a chain of one or more vertices (photographed 2 or more views) which occurred in sequence. This could be, for example,

$$K^- p \Rightarrow \Lambda\pi^+\pi^- , \quad \Lambda \rightarrow \pi^- p \qquad \text{or}$$
$$\Rightarrow K^0 p\pi^- , \quad K_1 \rightarrow \pi^- \pi^+$$
$$\Rightarrow \Sigma^0 \pi^+\pi^- , \quad \Sigma^0 \rightarrow \Lambda\gamma, \ \Lambda \rightarrow \pi^- p.$$

all of which exhibit two outgoing prongs at the production vertex, and a nearby V. We shall use this V-2 prong topology when giving program running times and output length.

2 The subroutined structure of PACKAGE has proven very adaptable to the needs of CUEST. Berkeley experience is that the amount of special coding for CUEST (about 2000 words) is comparable with the length of PACKAGE event-type programs for most experiments. Hence any laboratory which has a program equivalent to PACKAGE (stereo-reconstruction and kinematics in core together) should be able to replace the event type control program with the CUEST Program.

3 We assume that the variable are Gaussian distributed, unbiased, and have properly estimated uncertainties.

4 The easiest way to determine α^2 is to plot the experiment values of χ^2 on "probability paper" for χ^2 distributions. [for 4C, 3C, 2C, and 1C, these are available as Alvarez Memo 240 by J. Button-Shafer and A. H. Rosenfeld, Lawrence Radiation Laboratory, 1960 (unpublished)]. The scale on this paper is easily laid out so that proper χ^2 distribution fall on a straight line of unit slope. Real data tend to fall on a different straight line, with slope α^{-2}. Tables of the theoretical χ^2 distributions for C constraints can be found in any text on

statistics or in the Handbook of Chemistry and Physics, where C is called "Degrees of Freedom."

5 Note that this corresponds to about one minute/event, whereas Table III shows a sub-total of 12 sec/event! See Table IV for further discussion.

6 A single quadrupole acts like a cylindrical lens, and so may be used to distort a spot into a line about some axis, say horizontal. By reversing the currents one can make the line vertical, but one cannot achieve 45°. But the addition of four more poles permits arbitrary control of the axis direction.

7 SMP programs (12,000 words) are presently written in a combination of Fortran and 709 machine language, so for a PDP-1, recoding would be needed. Nevertheless for our example we chose a PDP-1 since it can eventually be used to run PEPR control hardware. For discussion of small computers appropriate to SMP and PEPR, see J. H. Munson, Alvarez Memo 453 (unpublished, 1963).

REFERENCES

1. "Instrumentation for High-Energy Physics;" Nucl. Instru. Methods 20, 367-463 (1963).
2. Proceedings of Informal Meeting on Track Data Processing, (CERN, Geneva 1962).
3. For specific references and a more detailed description see Rosenfeld, A. H., Nucl. Instr. Methods 20, 422 (1963).
4. Miller, W. and Fulbright, H., A Review of Data Analysis Systems for Nuclear and High Energy Physics in AEC Laboratories, (Division of Research, Atomic Energy Commission, Washington 25, D. C. 1962).
5. Bradner, Hugh, Ann. Rev. Nucl. Sci. 10, (1960).
6. White, Howard S., Lawrence Radiation Laboratory Report UCRL-9475, (Nov. 1960) unpublished.
   Thorndike, Alan T., Data Reduction Computation, BNL Bubble Chamber Group Memo F-3 (Brookhaven National Lab., 1958) unpublished.
7. Proceedings of Informal Meeting on Track Data Processing (CERN, Geneva 1962), p. 5.
8. Moorhead, A., Programme for the Geometrical Reconstruction of Curved Tracks in a Bubble Chamber, p. 33, (CERN, Geneva 1960); Solmitz, F. T., Helix Fit to Track Images (Ecole Polytechnique, Paris, 1960), unpublished; Burren, J. W. and Sparrow, J., The Geometrical Reconstruction of Bubble Chamber Tracks, Rutherford Laboratory Report NIRL/R/14 (1963).
9. Solmitz, F. T., Helix Fit to Track Images (Ecole Polytechnique, Paris 1960), unpublished.
10. Bock, R., GRIND Manual, DD/EXP/62/10, (CERN, Geneva, 1962) unpublished.

11. Penny, S. J., Alvarez Programmer Note P-8 (Lawrence Radiation Laboratory, 1963) unpublished.

12. Gell-Mann, M., and Rosenfeld, A. H. in Ann. Rev. Nucl. Sci. 7, 407 (1957), Appendix C, give the proof for the T_i vs T_j case. Since T, M_{ij}^2, and cos θ are linearly related, the proof applies to the other combinations too. For further details see Kirz, J., Alvarez Memo 439 (Lawrence Radiation Laboratory, 1963) unpublished.

13. Maglic, B., Alvarez, L. W., Rosenfeld, A. H., and Stevenson, M. L. Phys. Rev. Letters 7, 178 (1961).

14. Blatt, J. M., and Weisskopf, V. F., Theoretical Nuclear Physics (John Wiley and Son, New York, 1952).

15. Chinowsky, W., Goldhaber, G., Goldhaber, S., Lee, W., and O'Halloran, T. Phys. Rev. Letters 9, 330 (1962).

16. Goldhaber, Gerson, Memo TG-7, (Lawrence Radiation Laboratory, 1963), unpublished.

17. Berge, J. Peter, Solmitz, F. T., and Taft, Horace D., Rev. Sci. Instr. 32, 538-548 (1961).

18. Reference Manual for KICK, UCRL-9099, (Lawrence Radiation Laboratory, 1961), unpublished.

19. Humphrey, William E. and Ross, Ronald R., Phys. Rev. Letters 127, 1305 (1962).

20. Watson, M. B., Ferro-Luzzi, M., and Tripp, Robert D., UCRL-10542 (Lawrence Radiation Laboratory, 1963), to be published.

21. Davidon, W. C., ANL-5990 (Rev.) (Argonne National Laboratory, 1959), unpublished.

22. The degree of similarity to the "ravine" method mentioned by A. A. Tyapkin at the Tenth Rochester Conference (1960) is not known. Minfun is based on a second-hand description of the Russian procedure.

23. For a further breakdown see Rosenfeld, A.H., Alston, M.H., and Munson, J. Alvarez Memo 429 (Lawrence Radiation Laboratory, 1963), unpublished.

24. Alvarez, L.W., Davey, P., Hulsizer, R., Snyder, J., Schwemin, A.J., and Zane, R., UCRL-10109, (Lawrence Radiation Laboratory, 1962) unpublished.

25. Rosenfeld, A. H. and Taft, H. D., Alvarez Memo 440 (Lawrence Radiation Laboratory, 1963), unpublished.

26. Hough, P.V.C., Progress Report of the BNL-FSD Analysis System, G-29, BCHP-03-0-E, (Brookhaven National Laboratory, 1963), unpublished.

27. McCormick, R. H. and Narisimhan, R., in Proceedings of Informal Meeting on Track Data Processing (CERN, Geneva 1962) p. 401.

28. Marr, R. B., Pasko, J. R., Rabinowitz, G. BNL 6866 (AMD 312), (Brookhaven National Laboratory, 1963), unpublished.

29. Dickens, C. R., Downton, M. W., White, H. S., Software Development for the FSD System, UCRL-10859, (Lawrence Radiation Laboratory, June 10, 1963).

30. White, Howard S., "Future Development based on FSD," in Proceedings of Informal Meeting on Track Data Processing (CERN, Geneva, 1962) p. 33.

31. There is little published material on PEPR. The hardware is outlined in the original MIT proposal to the USAEC, February, 1962, authored by I.A. Pless. The latest general summary of PEPR as a system is given by Rosenfeld and Taft in references 25 and 23. The PEPR groups at MIT and Berkeley have both written a series of reports.

32. Hough, P.V.C., Comparison of Rapid Data Processing Systems, G-32 (BCHP-03-0F), (Brookhaven National Laboratory, 1963), unpublished.

33. A Proposal for a Trillion Bit Memory (International Business Machines Yorktown Heights, New York, 1962), unpublished; Pless, I.A. and Rosenfeld, A. H., The Precision-Encoded Memory (PEM), MIT PEPR Engineering Note (Massachusetts Institute of Technology, 1963), unpublished.

FIGURE LEGENDS

Fig. 1. Normal flow of data through the Alvarez data-analysis system is shown on this diagram. For simplicity, the library program LINGO is not shown on this chart. Lingo would use information from the track, event, and experiment stages of the analysis to maintain an up-to-date record of the status of the experiment.

Fig. 2. Example of the use of QUEST, taken from Alston, et al., Rev. Sci. Instr. 34, 64 (1963). The photographs and corresponding sketch show an unusual event from an experiment. The following reactions take place (track number in parenthesis);

Vertex 1. $K^-(1) + p \rightarrow \Xi^-(8) + K^+(15)$

Vertex 2. $\Xi^-(8) + p \rightarrow \pi^+(2) + p(3) + \Xi^-(4)$

Vertex 3. $\Xi^-(4) \rightarrow \pi^-(5) + \Lambda(9)$

Vertex 4. $\Lambda(9) \rightarrow \pi^-(6) + p(7)$.

Tracks 1 through 7 are measured; neutral tracks 8 through 11 are inserted by the program from vertex measurements. The on-line typewriter output from the event is shown in (b). The underlined letters and numbers are those inserted by the operator; the rest of the printout is written by the computer. The basis operation in the QUEST analysis is the vertex fit. When the operator types in "VERTEX", the program prepares for a normal vertex. The operator can also type VERTXX to cause the incident track to be extended by a mean gap length before the fit, or VERTMM to initiate a missing-mass calculation. Next, the operator identifies the tracks that take part in the fit. Finally the computer returns a heading line followed by a line of information pertinent to the fit. In the heading line, "LC" is an abbreviation for the constraint class of the vertex.

Fig. 3. SUMX cathode-ray tube display of a Dalitz plot in mass-squared units for an experiment with ±3% spread in beam momentum. The envelopes correspond to beam momenta of 1.51 GeV/c plus 3% and 1.51 GeV/c minus 3%. Inside the area where the envelopes overlap, the population would be uniform if it followed Lorentz-invariant phase space. Instead we see two resonant bands. The envelopes are plotted automatically by the "skin" subroutine of SUMX.

Fig. 4. Variables used for a triangle plot of four-body final states.

Fig. 5. Scatter diagram of $M_{p\pi^+}$ versus $M_{K^+\pi^-}$ plotted for the reaction $K^+ + p \rightarrow K^+ + \pi^- + p + \pi^+$ (15). The triangular border represents the kinematical limits. Smooth curves have been drawn on the projections to represent the distribution expected in the absence of dynamic effects. N^*_{33} production is apparent in the $M_{p\pi^+}$ projection; the $K^+\pi^-$ projection indicates strong K^* production.

Fig. 6. (a) The distribution in m^2 for a π^+ is assumed to be a Gaussian centered at m^2_π (0.02 GeV/c^2) with an experimental half width also equal to 0.02 GeV/c^2. (b) The corresponding distribution plotted in m rather than m^2. It is distorted with its peak shifted to the right by 33 MeV. Imaginary values of m (corresponding to $m^2 < 0$) are plotted to the left of the origin.

Fig. 7. Variables entering into discussion of missing-mass calculation.

Fig. 8. Diagrammatic illustration of the MINFUN stepping procedure for a function of two variables. The starting point is M; the new minima at M', M'', ... are represented by dots on the "railroad track" along the bottom of the ravine. The value of the function is calculated not only at the minima, but also at the "oversteps" 0, 0 ..., and the "sidesteps" S, S .... Derivatives are calculated at the overstep points only. See text for notation and stepping logic.

Fig. 9. Cross section of SMP track-encoder mechanism. Important features are: (a) light ray incident from film projector, (b) motor rotor, (c) motor stator, (d) white viewing curtain, (e) periscope mirrors, (f) rotating drum with

magnetic recording, (g) photomultiplier tube, (h) light-collector assembly (follows motion of periscope assembly), (i) glass bench-mark plate (bench marks photographed onto emulsion), (j) magnetic recording pickup heads to detect drum azimuth, and (k) ball bearings.

Fig. 10. Schematic of optics for the flying spot digitizer. Important features are (a) light source, (b) motor, (c) 8 curved slits on a rotating disk, (d) fixed slit, (e) orthogonal-scan optical path, (f) sweep photomultiplier, (g) normal-sweep optical path, (h) picket-fence optical path, (i) picket fence, and (j) picket-fence photomultiplier.

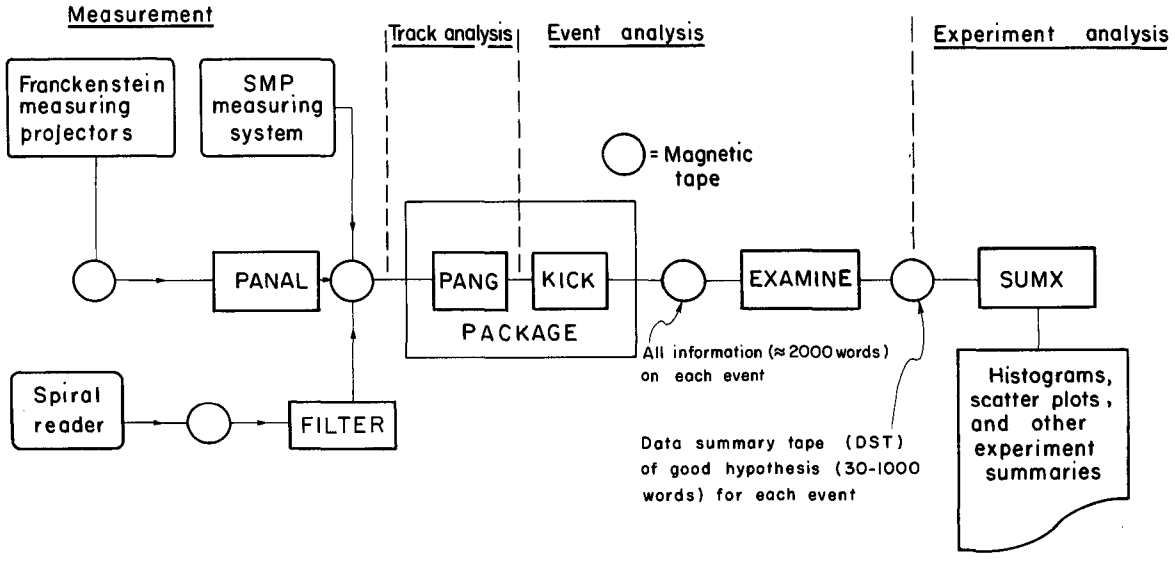
Measurement
Track analysis
Event analysis
Experiment analysis
Franckenstein measuring projectors
SMP measuring system
= Magnetic tape
PANAL
PANG
KICK
PACKAGE
EXAMINE
SUMX
Spiral reader
FILTER
All information (≈ 2000 words) on each event
Data summary tape (DST) of good hypothesis (30-1000 words) for each event
Histograms, scatter plots, and other experiment summaries
MU-31118

(a)

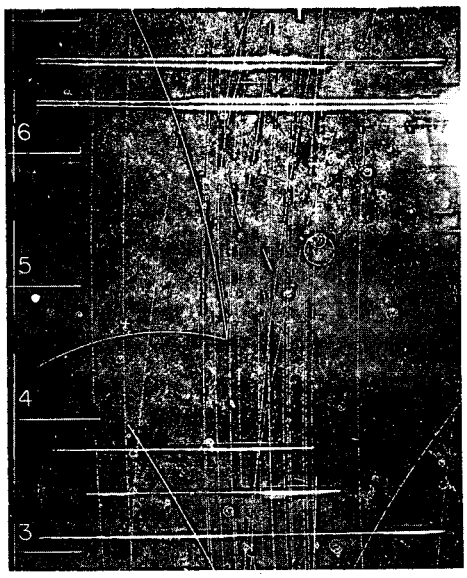

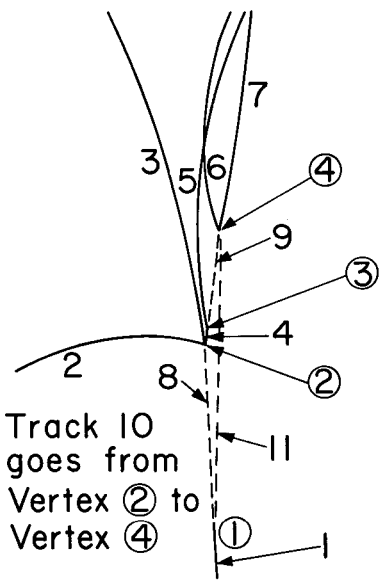

(b)

```
 THE FOLLOWING IS THE PACKAGE SUMMARY FOR THE TAPE LABELED INTERNALLY AS
 FOLLOWS.
        PANAL OUTPUT       FROM 9AP PANAL      620709
      72,07    ALVAREZ K72 TAPE 282 PREVUED 620703     SP Q EVTS FOR ALS
TON
CONTROL      000000000000  PR
HUNT
SERIAL NO FORMAT IS RRRRBBFFFBTT          3529  243 01
HUNTING FOR EVENT
CONTROL      3529  243 01  PR
IDENT
TOTAL NO. OF TRACKS IS  11,4
FORMAT IS TRACK N = LSZ,VERTEX,FUTURE VERTEX,CHARGE,MASS
TRACK  1 = L,1,0,-,K
TRACK  2 = L,2,0,+,PI
TRACK  3 = L,2,0,+,PR
TRACK  4 = L,2,3,-,XI
TRACK  5 = S,3,0,-,PI
TRACK  6 = L,4,0,-,PI
TRACK  7 = S,4,0,+,PR
TRACK  8 = Z,1,2,0,XI
TRACK  9 = Z,3,4,0,L
TRACK 10 = Z,2,4,0,L
TRACK 11 = Z,1,4,0,L
COMMENCING SPIFIT
COMMENCING MADFIT
  SERIAL 3529  243 01  TYPE 200 MEAS. 01 DATE MEAS. 62/07/02    PBEAM
  1510 DPBEAM     100     MAG  15.70  ORD       5
CONTROL      3529  243 01  PR
VERTEX
VERTEX TYPE = DECAY 3
TRACK 9
TRACK 6
TRACK 7
   CPM   HRJ   CHI SQ  LC LL       STEP   CUT   DAMN
     1          7.53  3  0          3     0     -0
IS EVENT GOOD      Y
NO OF TRACKS TO SWIM =  1
TRACK 9
CONTROL      3529  243 01  PR
VERTEX
VERTEX TYPE = DECAY 3
TRACK 4
TRACK 7
TRACK 9
   CPM   HRJ   CHI SQ  LC LL       STEP   CUT   DAMN
     2          1.06  3  0          3     0     0
IS EVENT GOOD      Y
NO OF TRACKS TO SWIM =  1
TRACK 4
CONTROL      3529  243 01  PR
VERTEX
VERTEX TYPE = PROD 4
TRACK 8
TRACK 2
TRACK 3
TRACK 5
NO OF TRACKS TO EXTEND  1
TRACK 1,8
   CPM   HRJ   CHI SQ  LC LL       STEP   CUT   DAMN
     3          1.67  3  0          2     0     -0
IS EVENT GOOD      Y
NO OF TRACKS TO SWIM =  0
CONTROL      3529  243 01  PR
STORE
NO OF TRACKS TO STORE  1
TRACK 8
CONTROL      3529  243 01  PR
VERTMM
VERTEX TYPE = PROD 2
TRACK 8
TRACK 3
   CPM        MMASS      DMMASS
     4      1536.64        2.72
IS EVENT GOOD      Y
NO OF TRACKS TO SWIM =  0
CONTROL      3529  243 01  PR
SWIM
NO OF TRACKS TO SWIM =  1
TRACK 8
CONTROL      3529  243 01  PR
VERTEX
VERTEX TYPE = PROD 3
TRACK 1
TRACK 8
TRACK 16=K
DO YOU WANT BEAM AVERAGE  Y
   CPM   HRJ   CHI SQ  LC LL       STEP   CUT   DAMN
     5          .09  1  0          2     0     -0
IS EVENT GOOD      Y
NO OF TRACKS TO SWIM =  0
CONTROL      3529  243 01  PR
DESTROY
NO OF TRACKS TO DESTROY = 0
ALL PUBS DESTROYED
CONTROL      3529  243 01  PR
VERTEX
VERTEX TYPE = DECAY 3
TRACK 11
TRACK 6
TRACK 7
   CPM   HRJ   CHI SQ  LC LL       STEP   CUT   DAMN
     6          1370  3  0          5     0     0
IS EVENT GOOD      N
CONTROL      3529  243 01  PR
END
DO YOU WANT AM END PRINT  Y
EVENT FINISHED
CONTROL       NONE  NONE   PR
BEED
YOU HAVE MADE AN ERROR
CONTROL       NONE  NONE   PR
BEAD
EVENT REJECT
  SERIAL 3680  224 01  TYPE 200 MEAS. 01 DATE MEAS. 62/07/01     PNLRJ
26 EVENT DISCARD CONTINUITY          ORD       6      CONTROL     3680  224 08
```

MUB-1291

Fig. 2

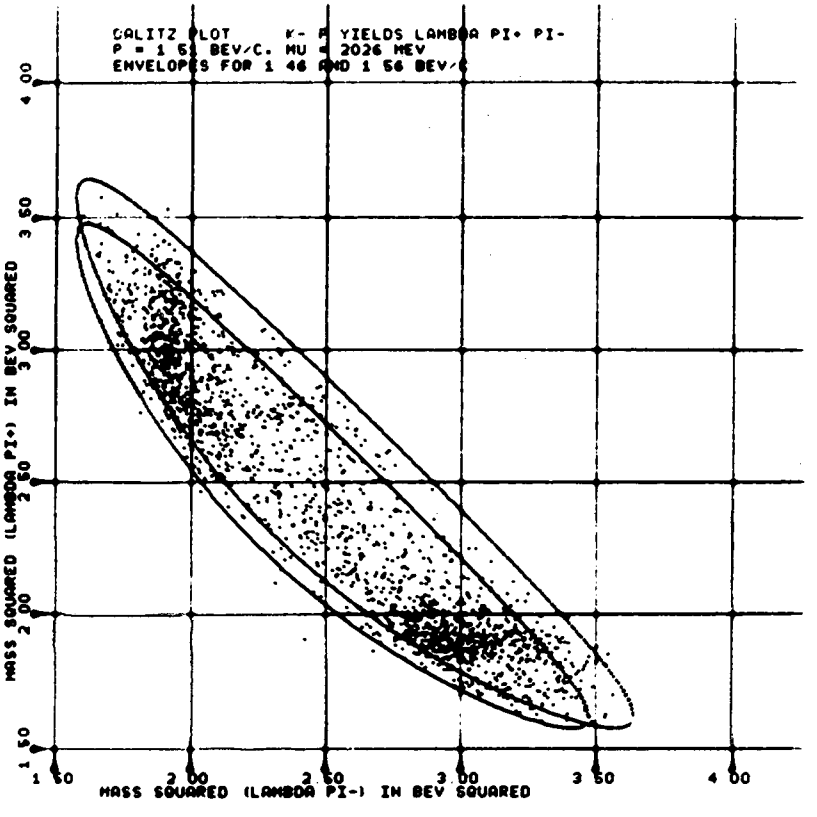

MU-30903

Fig. 3

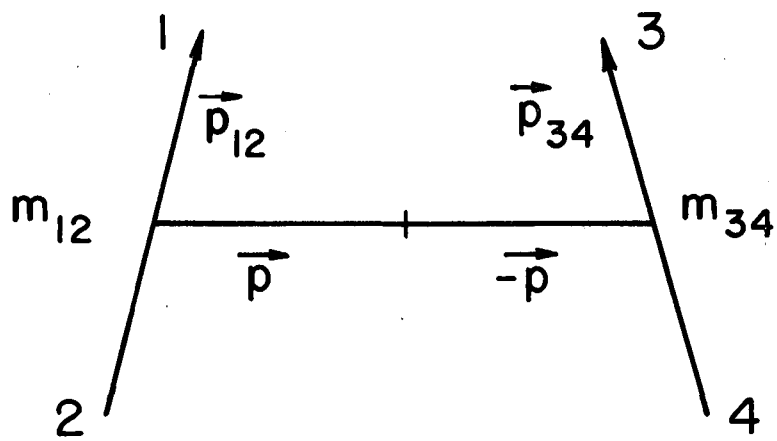

MU-30831

Fig. 4

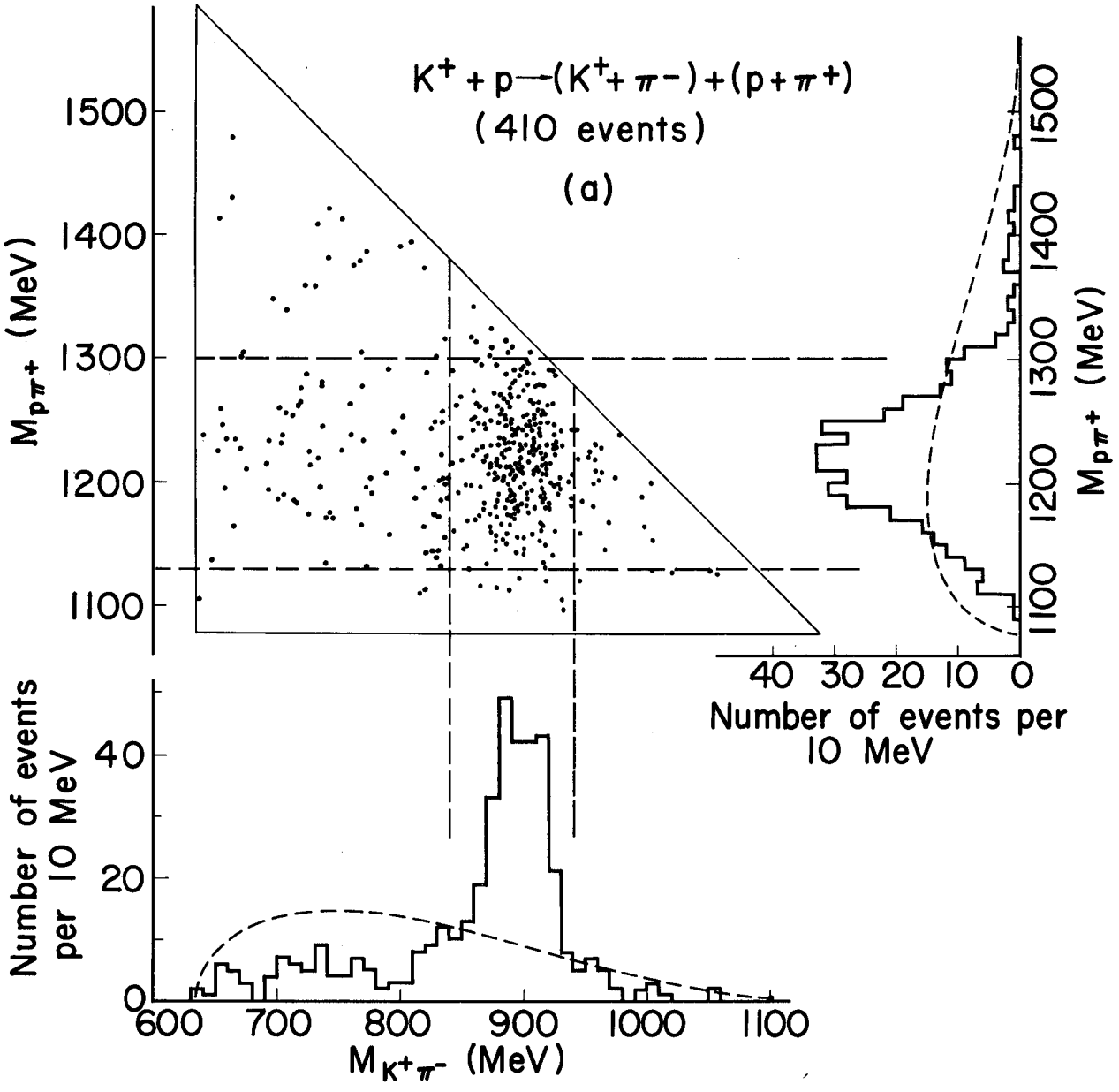

MUB-1560

Fig. 5

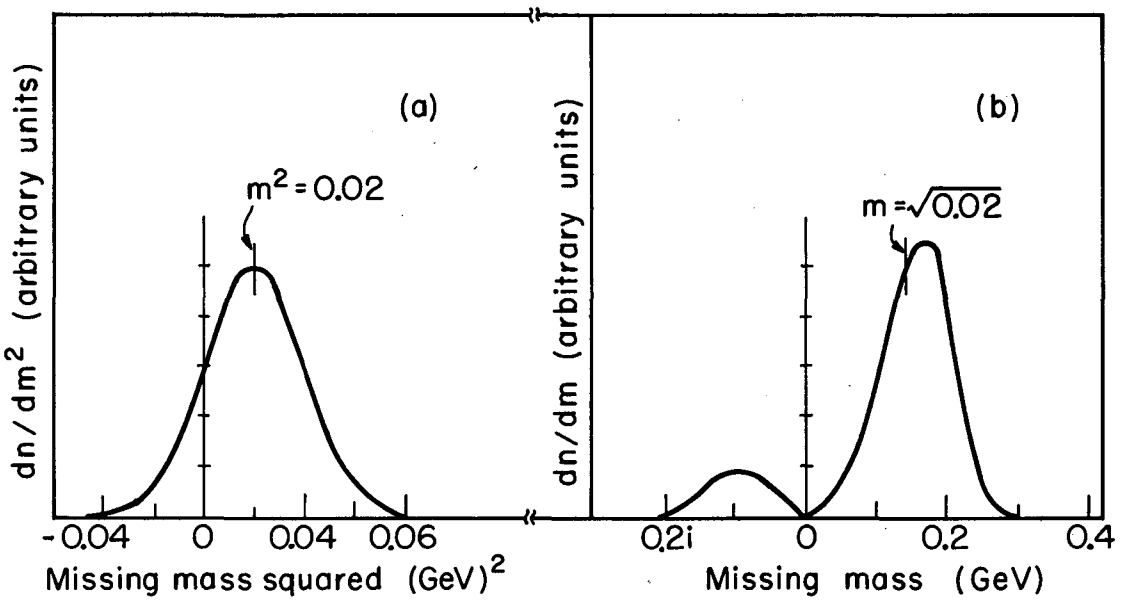
(a)
$m^2 = 0.02$
dn/dm^2 (arbitrary units)
-0.04
0
0.04
0.06
Missing mass squared $(GeV)^2$
(b)
$m = \sqrt{0.02}$
dn/dm (arbitrary units)
0.2i
0
0.2
0.4
Missing mass (GeV)
MU-30832

Fig. 6

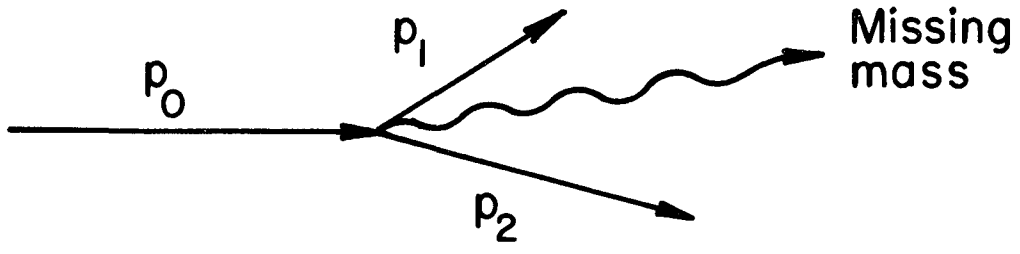

MU-30833

Fig. 7

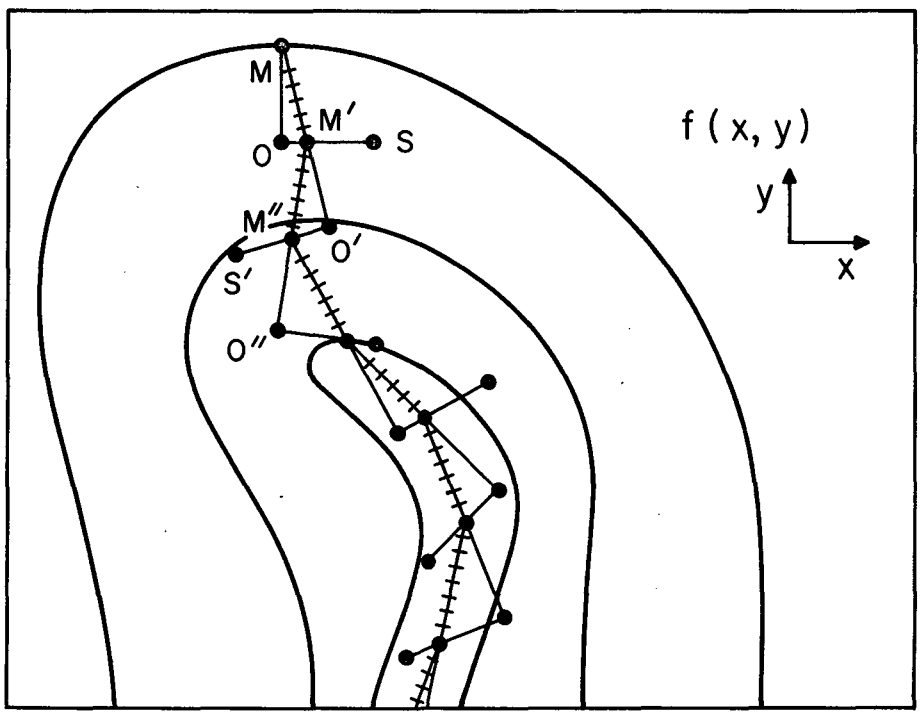

MU-30948

Fig. 8

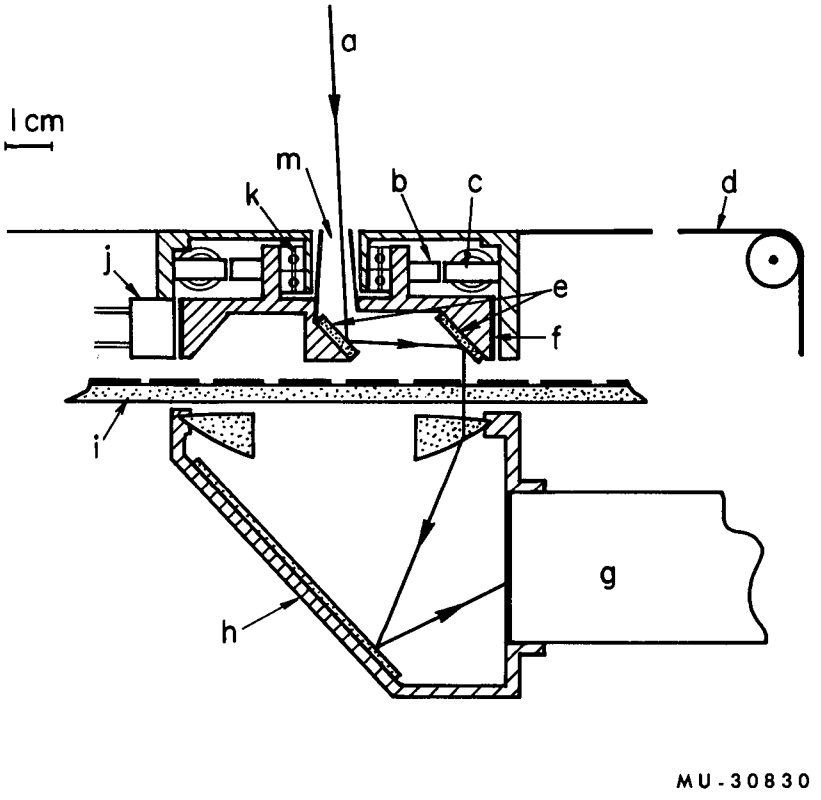

Fig. 9

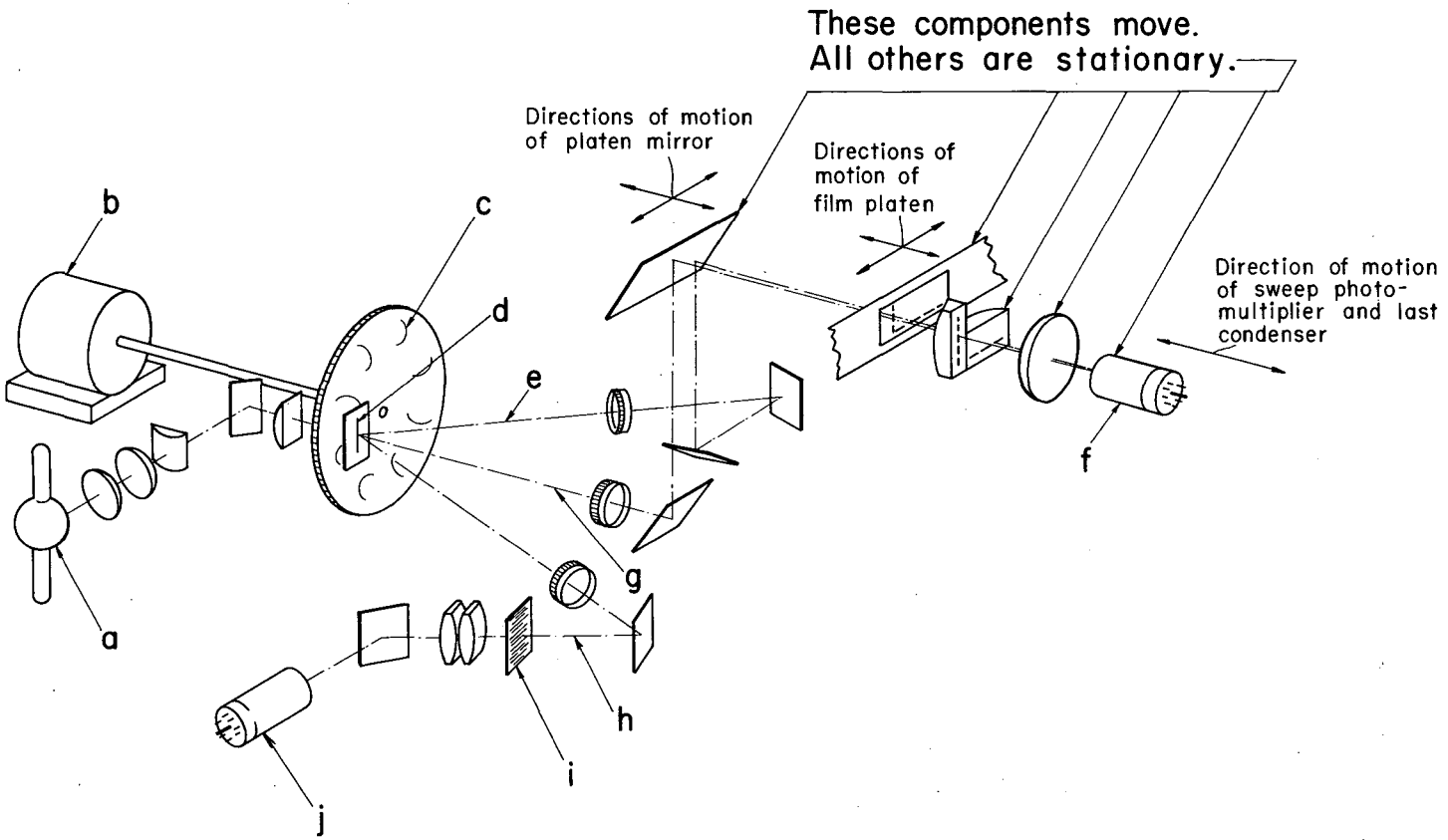
These components move.
All others are stationary.
Directions of motion of platen mirror
Directions of motion of film platen
Direction of motion of sweep photo-multiplier and last condenser
a
b
c
d
e
f
g
h
i
j
MUB-1920

Fig. 10